Empirical predictions of α-decay and spontaneous fission half-lives in the decay chains of elements 119 and 120

N. S. Moiseev[1,2] N. V. Antonenko[1,2] G. G. Adamian[1†]

[1]Bogoliubov Laboratory of Theoretical Physics, Joint Institute for Nuclear Research, 141980 Dubna, Russia
[2]School of Nuclear Science and Engineering, National Research Tomsk Polytechnic University, 634050 Tomsk, Russia

Abstract: The competition between α decay and spontaneous fission in the decay chains of isotopes with $Z = 119$ and 120 is investigated using empirical formulas. The α-decay half-lives are calculated with the Viola-Seaborg semi-empirical formula, whereas the spontaneous-fission half-lives are evaluated using an empirical formula based on the neutron excess N-Z and the α-decay energy Q_α. The reliability of this approach is validated by comparison with experimental data for known nuclei with $Z \geq 103$. Several α-decay chains are identified as promising candidates for experimental observation, with six or more consecutive α decays expected before termination by spontaneous fission. The present results may be useful for future experimental searches for superheavy nuclei.

Keywords: superheavy nuclei, alpha decay, spontaneous fission, empirical formulas, decay chains

DOI: **CSTR:**

CPC Accepted

I. Introduction

Alpha decay and spontaneous fission (SF) are the principal decay modes of heavy and superheavy nuclei (SHN) [1−7]. The unambiguous identification of new isotopes is greatly facilitated by the observation of their α-decay chains terminating in SF. Experimental and theoretical investigations of these nuclei constitute a major frontier in modern nuclear physics [8−21]. Consequently, a comprehensive understanding of the competition between α decay and SF is indispensable for guiding experimental exploration and accurately mapping the extent and boundaries of the island of stability [1−3, 22−30].

Although various microscopic approaches have been developed to describe α decay [31−35] and SF [36−42], their application to heavy and superheavy systems remains computationally demanding and sensitive to uncertainties in shell structure and fission barrier heights. These challenges have sustained strong interest in developing fast semi-empirical methods for systematic half-life predictions [43−55].

For α decay, the Viola–Seaborg relation [45] remains a widely used semi-empirical tool. It is commonly expressed as

$$\log_{10} T^{\alpha}_{1/2}\,(\mathrm{s}) = \frac{aZ+b}{\sqrt{Q_\alpha}} + cZ + d + h_\alpha, \qquad (1)$$

where Z is the proton number and Q_α is the α-decay energy. In this work, we adopt the Parkhomenko–Sobiczewski parameterization [56], which, as demonstrated in Ref. [57], provides high accuracy for SHN when benchmarked against experimental $T^{\alpha}_{1/2}$ data. The corresponding coefficients are $a = 1.3892$, $b = 13.862$, $c = -0.1086$, and $d = -41.458$, while $h_\alpha = 0$, 0.437, 0.641, and 1.024 for even-even, odd-even, even-odd, and odd-odd nuclei, respectively.

For SF half-lives, we have previously found that, at fixed $N-Z$, $\log_{10} T^{\mathrm{SF}}_{1/2}$ depends nearly linearly on Q_α [58, 59]. This observation enabled us to derive an empirical formula that relates SF half-lives directly to the α-decay energy Q_α and the neutron excess $N-Z$:

$$\log_{10} T^{\mathrm{SF}}_{1/2}\,(\mathrm{s}) = c_0 + c_1(N-Z) + c_2(N-Z)^2 + c_Q Q_\alpha + h_{\mathrm{SF}}, \qquad (2)$$

where $h_{\mathrm{SF}} = 0$, h, and $1.575h$ for even-even, odd-A, and odd-odd nuclei, respectively. The coefficients are divided into two sets according to Z: for $90 \leq Z \leq 102$, $c_0 = -244.845$, $c_1 = 12.2843$, $c_2 = -0.12658$, $c_Q = -6.1023$, and $h = 4.309$; for $Z \geq 103$, $c_0 = -0.414$, $c_1 = 0.1379$, $c_2 = 0$, $c_Q = -0.9097$, and $h = 2.327$. Because Eq. (2) uses only Q_α, which is typically determined more reliably than absolute masses or shell-correction energies [60], it avoids the model-dependent uncertainties inherent in microscopic fission calculations.

Most heavy and superheavy nuclei are deformed, and deformation can affect both α-decay and SF half-lives.

Received 30 August 2026; Accepted 29 October 2026

† E-mail: adamian@theor.jinr.ru

©2026 Chinese Physical Society and the Institute of High Energy Physics of the Chinese Academy of Sciences and the Institute of Modern Physics of the Chinese Academy of Sciences and IOP Publishing Ltd. All rights, including for text and data mining, AI training, and similar technologies, are reserved.

Explicitly incorporating quadrupole and hexadecapole deformation parameters into the generalized liquid drop model has been shown to improve agreement with experimental data, particularly in the superheavy region [61]. Because the ground-state masses of the parent and daughter nuclei depend on their shapes, deformation is partially embedded in the α-particle separation energy Q_α. In the present work, therefore, deformation is treated implicitly through Q_α.

The aim of the present work is to investigate the competition between α decay and SF along the α-decay chains of $Z = 119$ and $Z = 120$ isotopes, whose properties are currently the subject of intensive experimental and theoretical studies. For this purpose, we employ Eq. (1) and Eq. (2) to estimate the corresponding half-lives for nuclei in the α-decay chains of $Z = 119$ isotopes with $A =$ 293–298 and $Z = 120$ isotopes with $A =$ 295–300, extending down to Lr and Rf isotopes. The corresponding neutron-excess values, $N - Z = 55$ to 60, place these nuclei near the predicted island of stability, making their decay characteristics particularly relevant for guiding future experimental efforts at the limits of the nuclear chart. The novelty of the present work lies in its systematic mapping of this competition and its identification of robust experimental decay chains.

II. General trends in α-decay and SF competition

To obtain an overall picture of the competition between α decay and SF in the region of interest, we first calculate the partial half-lives using the formulas described above. The α-decay half-life $T^{\alpha}_{1/2}$ is obtained from Eq. (1), whereas the SF half-life $T^{\mathrm{SF}}_{1/2}$ is calculated using Eq. (2). Both formulas require the α-decay energy Q_α as input.

The calculations use experimental Q_α values from Ref. [62] whenever available; otherwise, the values are taken from the macroscopic–microscopic model of Ref. [63]. This model combines the Yukawa-plus-exponential macroscopic energy [64] with microscopic shell and pairing corrections obtained via the Strutinsky method from the single-particle levels of a deformed Woods–Saxon potential. It is widely used in this mass region and provides calculated Q_α values for all nuclei of interest. To quantify its accuracy, we define the deviation for Q_α as $\delta^{Q_\alpha} = Q_\alpha^{\mathrm{calc.}} - Q_\alpha^{\mathrm{exp.}}$. Its performance against the experimental Q_α data from Ref. [62] is characterized by a mean deviation (indicating overestimation) of $\langle \delta^{Q_\alpha} \rangle = 136$ keV, a mean absolute deviation of $\langle |\delta^{Q_\alpha}| \rangle = 260$ keV, and a root-mean-square deviation of $\delta^{Q_\alpha}_{\mathrm{rms}} = 315$ keV, evaluated for 92 nuclei with $Z \geq 103$.

To assess the quality of the description, the calculated half-lives for both decay modes are compared with experimental data. For α-decay half-lives, the primary source is Ref. [7], supplemented by the most recent experimental data for ^{272}Hs, ^{275}Ds [13], ^{276}Ds [12], and ^{257}Sg [15]. The ground-state half-lives of ^{261}Rf, ^{265}Sg, ^{271}Hs, and ^{273}Ds are updated according to the one-quasiparticle level schemes proposed in Ref. [13]. Additional data for ^{251}Lr [65], ^{253}Rf [30], ^{257}Db [66], ^{268}Db [9, 11], ^{272}Bh, $^{282-285}$Nh and ^{286}Mc [11], ^{258}Sg [67], ^{262}Sg [68], ^{264}Sg [25], ^{269}Sg, ^{281}Cn, ^{289}Lv [69], ^{288}Lv [70], ^{271}Sg, ^{275}Hs, ^{283}Cn, ^{286}Fl [10], ^{265}Bh [71], ^{264}Hs [29], ^{267}Hs [24], ^{273}Hs [72], ^{282}Mt, ^{286}Rg, ^{284}Fl [23], and ^{284}Cn [20] are also included, with half-lives and branching ratios (or their limits) taken from the original publications or updated as necessary.

For SF half-lives, experimental values are taken primarily from Refs. [7, 29], together with the recently reported half-lives of ^{252}Rf [14], ^{263}Rf [13], ^{264}Lr [9, 11], ^{257}Db [66], ^{266}Db [11], ^{257}Sg [15], ^{268}Sg, and ^{276}Ds [12]. In addition, the data for ^{255}Lr [73], ^{267,268}Db, ^{279,281}Rg, ^{285}Nh [11], ^{277}Mt [74], ^{259}Sg [75], ^{269}Sg, ^{281}Cn [69], ^{260}Bh [76], ^{265}Hs [77], ^{270}Hs [78], ^{275}Hs [10], and ^{284}Fl [23] are updated or supplemented, including branching ratios and half-life limits where applicable.

To validate the use of theoretical Q_α values from Ref. [63] in the present calculations, we compare the resulting half-lives with experimental data. Nuclei for which only limits are available were excluded from the statistical analysis. For each decay mode m ($m = \alpha$ or SF), we define the deviation as $\delta^{T^m_{1/2}} = \log_{10}(T^{m,\mathrm{calc.}}_{1/2}/T^{m,\mathrm{exp.}}_{1/2})$. For 120 nuclei with $Z \geq 103$ and known experimental α-decay half-lives, the use of theoretical Q_α values in Eq. (1) yields a mean absolute deviation $\langle |\delta^{T^{\alpha}_{1/2}}| \rangle = 0.80$ orders of magnitude and a root-mean-square deviation $\delta^{T^{\alpha}_{1/2}}_{\mathrm{rms}} = 1.10$. For 59 nuclei with $Z \geq 103$ and known experimental SF half-lives, the same Q_α input in Eq. (2) gives $\langle |\delta^{T^{\mathrm{SF}}_{1/2}}| \rangle =$ 0.97 orders of magnitude and $\delta^{T^{\mathrm{SF}}_{1/2}}_{\mathrm{rms}} = 1.40$. These deviations are within the typical accuracy of empirical systematics and confirm that the formulas reproduce the overall magnitudes of the half-lives. We therefore use theoretical Q_α values for all nuclei for which experimental values are unavailable.

Figure 1 presents contour maps of the logarithms of the calculated half-lives for SF and α decay of even-even nuclei in the region $104 \leq Z \leq 120$ and $46 \leq N - Z \leq 64$. The calculations use Q_α values obtained from Ref. [63]. The half-lives exhibit smooth trends, decreasing gradually with decreasing neutron excess and increasing proton number. In contrast to shell-correction energies, which typically exhibit pronounced structures around magic numbers [79–81], the half-lives vary more smoothly across the considered region. Although the formulas used for both decay modes do not explicitly include shell corrections, shell-structure information enters through the Q_α values and is reflected in the observed half-life variations. An increase in both SF and α-decay half-lives is observed near the deformed shell closure at $N = 162$. Within the present semi-empirical description, the en-

CPC Accepted

hancement of the half-lives associated with this shell closure is less pronounced for SF than for α decay.

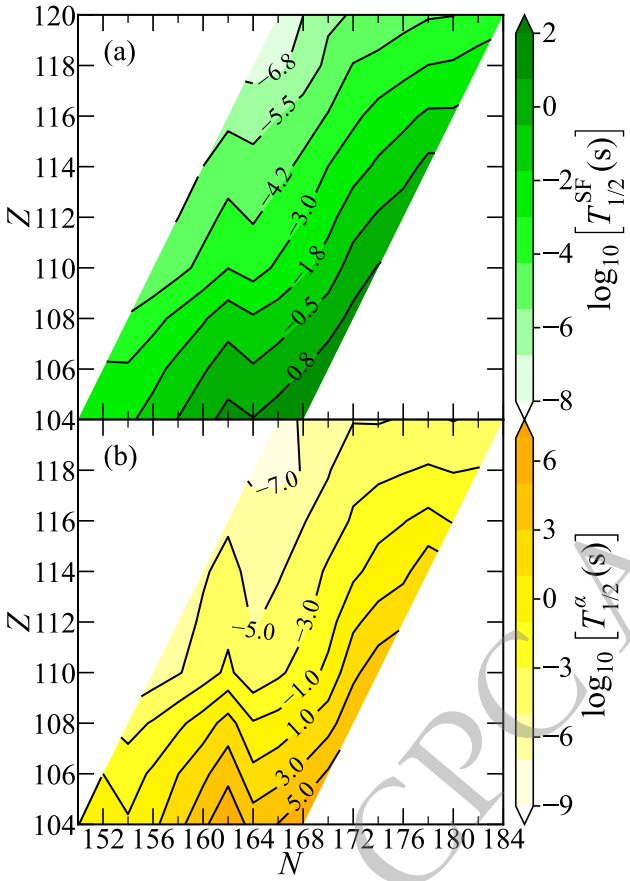


Fig. 1. (color online) Color contour maps show the logarithms of SF (a) and α-decay (b) half-lives, expressed in seconds, for even-even nuclei with proton numbers $104 \le Z \le 120$ and neutron excess $46 \le N-Z \le 64$. The half-lives were calculated using Eq. (1) for α decay and Eq. (2) for SF, with Q_α values from Ref. [63].

Figures 2 and 3 present the calculated partial half-lives for α decay and SF along the α-decay chains of $Z = 119$ and $Z = 120$ isotopes, respectively, in comparison with experimental data. Experimental Q_α values from Ref. [62] are used where available; otherwise, theoretical Q_α values from Ref. [63] are employed.

A global trend observed in both figures is the decrease in the partial half-lives for both decay modes as one moves further into the superheavy region. The extent to which one decay mode dominates over the other can be assessed from the vertical separation between the two corresponding curves: the larger the separation, the higher the probability of decay through the mode with the shorter half-life.

For chains starting from ^{293,294,296}119 and ^{295}120, α decay clearly dominates over SF by about two orders of magnitude at the initial members of the chains. However, this behavior changes abruptly at neutron number $N = 162$, where the α-decay half-lives increase sharply, whereas the SF half-lives exhibit a much less pronounced increase. Consequently, SF becomes the dominant decay mode for $N < 162$. In contrast, for chains starting from ^{295,297,298}119 and ^{297,299}120, the two decay modes already exhibit strong competition from the initial steps of the chains, with SF clearly dominating for $N < 162$. For chains initiated by ^{296,298,300}120, SF dominates almost immediately. A particularly prominent feature is observed at $N = 172$, where the α-decay half-lives increase more substantially than the SF half-lives, leading to pronounced SF dominance.

Comparing the two elements, the half-lives of $Z = 119$ isotopes are systematically longer than those of $Z = 120$ isotopes. Odd-even effects are also evident: for even-Z-odd-N nuclei, the SF half-lives are noticeably longer than those of even-even nuclei, whereas the α-decay half-lives show much weaker sensitivity to these effects.

To further assess the predictive power of the approach, we compare the calculated dominant decay modes with experimental data for 64 nuclei with $103 \le Z \le 118$ and $261 \le A \le 295$. This set comprises the nuclei for which at least one partial half-life of the two considered decay modes is experimentally known with sufficient accuracy for a quantitative comparison. The full comparison of the calculated and experimental half-lives and branching ratios is given in Table 1 of Appendix A, which also includes two additional nuclei for which only limits on the branching ratios are available. The predicted dominant decay mode agrees with experiment in 53 cases. The remaining 11 discrepancies are discussed below and grouped according to the predicted dominant mode.

For ^{277}Mt and ^{279,281}Rg, α decay is predicted to dominate. For ^{277}Mt, only SF has been observed, whereas for ^{279}Rg and ^{281}Rg, the available experimental data on both modes indicate competition between α decay and SF. Microscopic calculations of $T^{SF}_{1/2}$ are not available for these three nuclei. For ^{281}Rg, the WS4 model [82, 83] gives $Q_\alpha = 9.76$ MeV, which is 0.60 MeV lower than the value used here, and the corresponding $T^{\alpha,calc.}_{1/2} = 8.4$ s is only about one order of magnitude smaller than the experimental value $T^{\alpha,exp.}_{1/2} = 79$ s. For ^{277}Mt, all considered models [63, 81, 83] give $T^{SF,calc.}_{1/2} \sim 10$ s, which is three to four orders of magnitude larger than $T^{SF,exp.}_{1/2} = 5.0$ μs. For ^{279}Rg, the values calculated with Q^{exp}_α favour α decay but differ only by a factor of 19, which is still consistent with the experimentally observed competition.

For ^{286,288}Fl and ^{288,290,292}Lv, SF is predicted to dominate. For ^{286}Fl, the available experimental data on both modes indicate competition between α decay and SF,

CPC Accepted

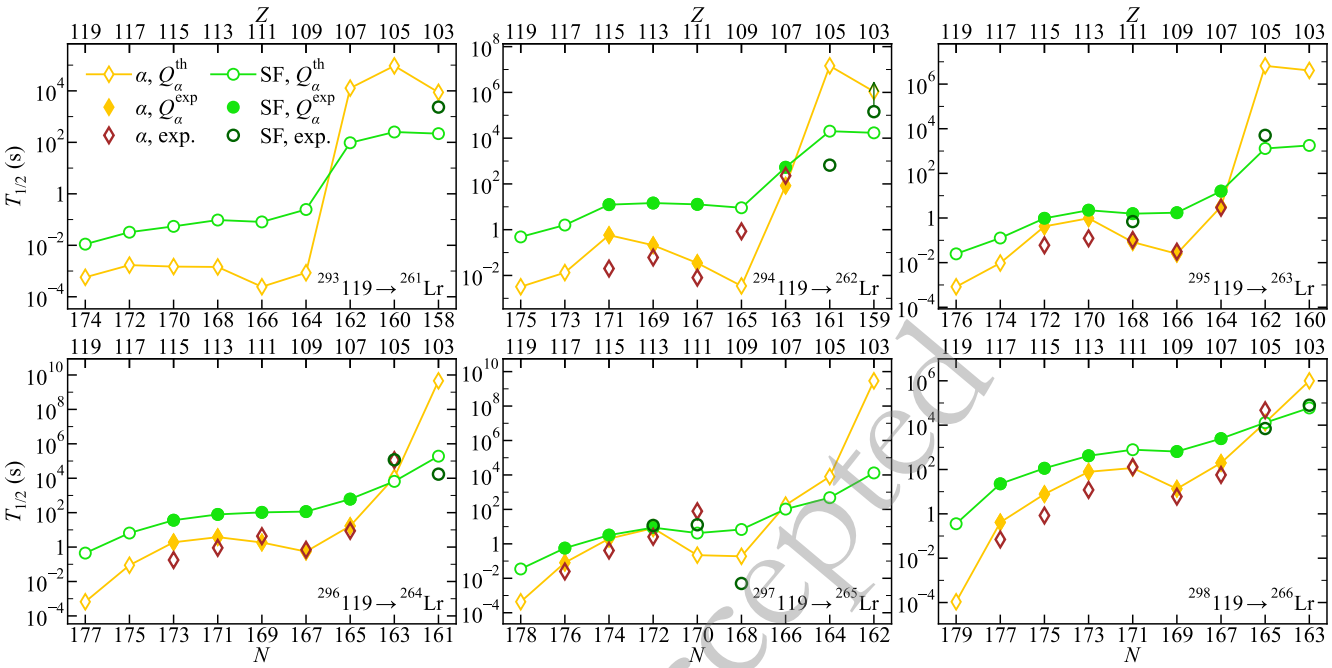


Fig. 2. (color online) Comparison of the calculated α-decay (yellow diamonds connected by lines) and SF (green circles connected by lines) half-lives for α-decay chains originating from isotopes of element 119 with mass numbers A = 293–298. The α-decay and SF half-lives are calculated using Eq. (1) and Eq. (2), respectively. Solid symbols denote calculations based on experimental Q_α values from Ref. [62], whereas open symbols denote calculations based on theoretical Q_α values from Ref. [63]. Experimental α-decay (open brown diamonds) and SF (open darkgreen circles) half-lives are taken from Refs. [7, 29]. Downward (upward) arrows indicate upper (lower) limits on the half-life for the corresponding decay mode.

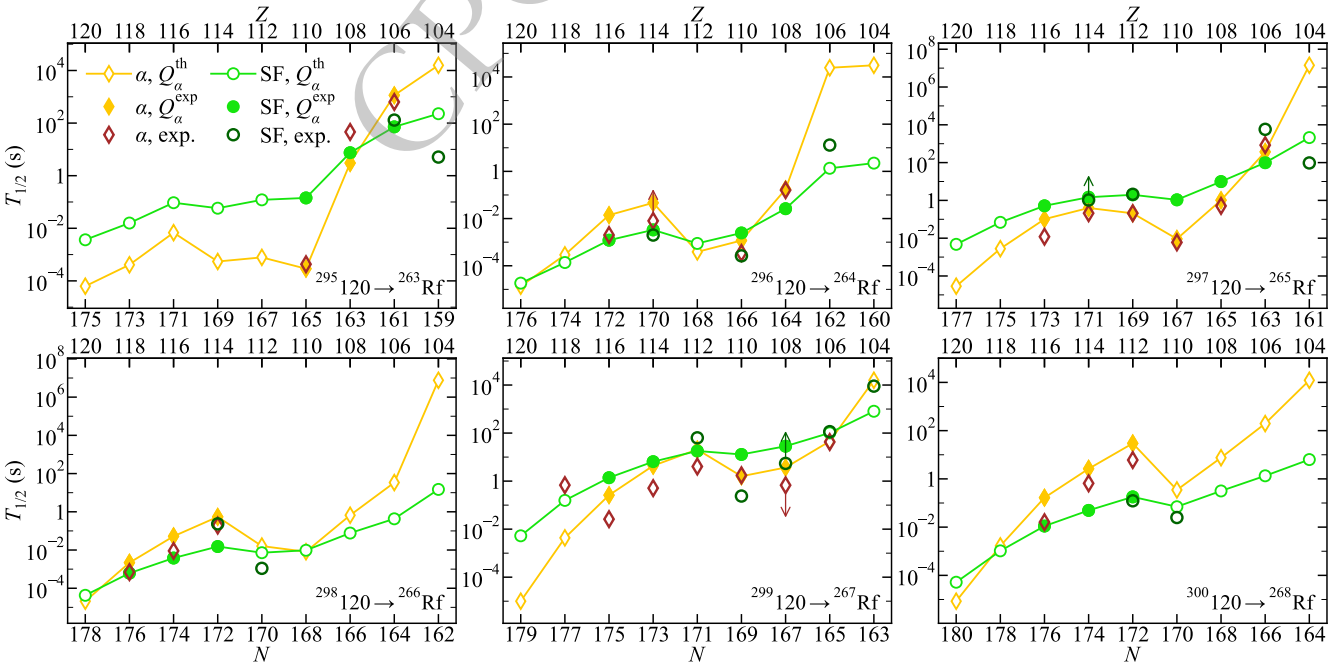


Fig. 3. (color online) Same as in Fig. 2, but for the α-decay chains of Z = 120 isotopes with mass numbers A = 295–300.

whereas for ^{288}Fl and the Lv isotopes, only α decay has been detected so far. The microscopic models show considerable disagreement for these nuclei when compared with the $T^{\alpha}_{1/2}$ values calculated from Q^{exp}_{α} using Eq. (1). For ^{288}Fl, Ref. [84] predicts SF dominance, whereas Refs. [36, 38] favour α decay. For ^{286}Fl and ^{288}Lv, Ref. [39] predicts SF dominance, Refs. [36–38] favour α decay, and Ref. [84] predicts competition. For ^{292}Lv and ^{290}Lv,

CPC Accepted

Table 1. Comparison of calculated and experimental half-lives for 66 nuclei with atomic numbers $103 \le Z \le 118$ and neutron excesses $55 \le N-Z \le 60$. The first column lists the nucleus. The second column gives the Q_α values; values in roman typeface are experimental data from Ref. [62], whereas values in italics are theoretical Q_α values taken from Ref. [63]. Q_α values marked with an asterisk are taken from the reference listed in the last column. Columns 3 to 7 contain the calculated total half-life (considering only α decay and SF), the α-decay and SF branching ratios, and the corresponding partial half-lives $T_{1/2}^{\alpha,\mathrm{calc.}}$ and $T_{1/2}^{\mathrm{SF,calc.}}$. The partial α-decay half-life is obtained using Eq. (1), and the SF half-life is obtained using Eq. (2). Columns 8 to 12 list the corresponding available experimental quantities: the total half-life $T_{1/2}^{\mathrm{exp.}}$, branching ratios $b_{\alpha,\mathrm{exp.}}$ and $b_{\mathrm{SF,exp.}}$, and partial half-lives $T_{1/2}^{\alpha,\mathrm{exp.}}$ and $T_{1/2}^{\mathrm{SF,exp.}}$. The last column provides references for the experimental data.

Nuclide	Q_α (MeV)	$T_{1/2}^{\mathrm{calc.}}$	$b_{\alpha,\mathrm{calc.}}$ (%)	$b_{\mathrm{SF,calc.}}$ (%)	$T_{1/2}^{\alpha,\mathrm{calc.}}$ (s)	$T_{1/2}^{\mathrm{SF,calc.}}$ (s)	$T_{1/2}^{\mathrm{exp.}}$	$b_{\alpha,\mathrm{exp.}}$ (%)	$b_{\mathrm{SF,exp.}}$ (%)	$T_{1/2}^{\alpha,\mathrm{exp.}}$ (s)	$T_{1/2}^{\mathrm{SF,exp.}}$ (s)	References
^{261}Lr	*7.87*	3.54 min	2.4	97.6	8.8×10^{3}	2.2×10^{2}	39 min		≈100		2.3×10^{3}	[7]
^{262}Lr	*7.41*	4.67 h	1.5	98.5	1.1×10^{6}	1.7×10^{4}	≈4 h		<10		$>1.4\times10^{5}$	[7]
^{264}Lr	*6.56*	2.21 d	0.004	100.0	4.6×10^{9}	1.9×10^{5}	4.8 h		100		1.7×10^{4}	[11]
^{266}Lr	*7.42*	15.6 h	5.6	94.4	1.0×10^{6}	6.0×10^{4}	22 h		100		7.9×10^{4}	[7]
^{263}Rf	*7.85*	3.73 min	1.4	98.6	1.6×10^{4}	2.3×10^{2}	5.1 s		100		5.1	[13]
^{265}Rf	*7.09*	35.1 min	0.01	100.0	1.4×10^{7}	2.1×10^{3}	1.6 min		≈100		9.6×10^{1}	[7]
^{267}Rf	*7.85*	12.8 min	4.9	95.1	1.6×10^{4}	8.1×10^{2}	2.5 h		100		9.0×10^{3}	[7]
^{266}Db	*7.33*	5.60 h	0.1	99.9	1.4×10^{7}	2.0×10^{4}	11 min		100		6.6×10^{2}	[11]
^{267}Db	*7.32*	21.7 min	0.02	100.0	6.6×10^{6}	1.3×10^{3}	1.4 h		100		5.0×10^{3}	[11]
^{268}Db	*8.17*	1.14 h	37.2	62.8	1.1×10^{4}	6.6×10^{3}	16 h	51	49	1.1×10^{5}	1.2×10^{5}	[11]
^{270}Db	*8.15*	1.80 h	49.9	50.1	1.3×10^{4}	1.3×10^{4}	1.7 h	≈13	≈87	4.7×10^{4}	7.0×10^{3}	[7]
^{267}Sg	8.40*	1.13 min	5.9	94.1	1.1×10^{3}	7.2×10^{1}	1.8 min	17	83	6.4×10^{2}	1.3×10^{2}	[7]
^{268}Sg	*7.89*	1.35 s	0.01	100.0	2.5×10^{4}	1.4	13 s		100		1.3×10^{1}	[12]
^{269}Sg	8.55*	1.30 min	21.1	78.9	3.7×10^{2}	9.9×10^{1}	13 min	87	13	8.4×10^{2}	5.8×10^{3}	[69]
^{271}Sg	*8.84*	31.4 s	69.1	30.9	4.5×10^{1}	1.0×10^{2}	31 s	73	27	4.2×10^{1}	1.1×10^{2}	[10]
^{270}Bh	9.06	1.20 min	86.5	13.5	8.3×10^{1}	5.3×10^{2}	3.8 min	100		2.3×10^{2}		[7]
^{271}Bh	9.42	2.69 s	83.2	16.8	3.2	1.6×10^{1}	2.90 s	100		2.9		[7]
^{272}Bh	9.30	16.3 s	97.3	2.7	1.7×10^{1}	6.1×10^{2}	8.8 s	100		8.8		[11]
^{274}Bh	8.94	3.05 min	92.6	7.4	2.0×10^{2}	2.5×10^{3}	57 s	100		5.7×10^{1}		[7]
^{271}Hs	9.48*	2.15 s	71.2	28.8	3.0	7.5	46 s	100		4.6×10^{1}		[13]
^{272}Hs	9.77	22.8 ms	13.0	87.0	1.7×10^{-1}	2.6×10^{-2}	0.16 s	100		1.6×10^{-1}		[12]
^{273}Hs	9.65	927 ms	90.6	9.4	1.0	9.9	0.51 s	100		5.1×10^{-1}		[72]
^{275}Hs	9.45	3.25 s	88.5	11.5	3.7	2.8×10^{1}	0.60 s	>89	<11	$<6.7\times10^{-1}$	>5.5	[10]
^{274}Mt	*11.01*	3.48 ms	100.0	0.04	3.5×10^{-3}	9.1	850 ms	100		8.5×10^{-1}		[7]
^{275}Mt	10.48	24.5 ms	98.6	1.4	2.5×10^{-2}	1.7	31 ms	100		3.1×10^{-2}		[7]
^{276}Mt	10.10	543 ms	99.5	0.5	5.5×10^{-1}	1.2×10^{2}	700 ms	100		7.0×10^{-1}		[7]
^{277}Mt	*10.13*	184 ms	97.3	2.7	1.9×10^{-1}	6.8	5 ms		100		5.0×10^{-3}	[74]
^{278}Mt	9.58	13.2 s	98.0	2.0	1.3×10^{1}	6.5×10^{2}	6 s	100		6.0		[7]
^{275}Ds	11.37	290 μs	99.8	0.2	2.9×10^{-4}	1.4×10^{-1}	0.43 ms	100		4.3×10^{-4}		[13]
^{276}Ds	10.90	795 μs	67.5	32.5	1.2×10^{-3}	2.4×10^{-3}	0.15 ms	43	57	3.5×10^{-4}	2.6×10^{-4}	[12]
^{277}Ds	10.71	9.10 ms	99.2	0.8	9.2×10^{-3}	1.1	6 ms	≈100		6.0×10^{-3}		[7]
^{279}Ds	9.83	1.42 s	89.0	11.0	1.6	1.3×10^{1}	210 ms	12	88	1.8	2.4×10^{-1}	[7]
^{280}Ds	*9.91*	58.3 ms	16.7	83.3	3.5×10^{-1}	7.0×10^{-2}	25 ms		100		2.5×10^{-2}	[7]
^{278}Rg	10.85	34.7 ms	99.7	0.3	3.5×10^{-2}	1.3×10^{1}	8 ms	100		8.0×10^{-3}		[7]

CPC Accepted

Table 1-continued from previous page

Nuclide	Q_α (MeV)	$T_{1/2}^{\rm calc.}$	$b_{\alpha,\rm calc.}$ (%)	$b_{\rm SF,calc.}$ (%)	$T_{1/2}^{\alpha,\rm calc.}$ (s)	$T_{1/2}^{\rm SF,calc.}$ (s)	$T_{1/2}^{\rm exp.}$	$b_{\alpha,\rm exp.}$ (%)	$b_{\rm SF,exp.}$ (%)	$T_{1/2}^{\alpha,\rm exp.}$ (s)	$T_{1/2}^{\rm SF,exp.}$ (s)	References
^{279}Rg	10.53	79.0 ms	95.0	5.0	8.3×10^{-2}	1.6	90 ms	87	13	1.0×10^{-1}	6.9×10^{-1}	[11]
^{280}Rg	10.15	1.82 s	98.3	1.7	1.8	1.0×10^{2}	4.3 s	100		4.3		[7]
^{281}Rg	*10.36*	209 ms	95.0	5.0	2.2×10^{-1}	4.2	11 s	14	86	7.9×10^{1}	1.3×10^{1}	[11]
^{282}Rg	*9.49*	1.69 min	87.0	13.0	1.2×10^{2}	7.8×10^{2}	130 s	100		1.3×10^{2}		[7]
^{281}Cn	10.42*	187 ms	90.5	9.5	2.1×10^{-1}	2.0	0.19 s	91	9	2.1×10^{-1}	2.1	[69]
^{282}Cn	*10.69*	4.99 ms	31.0	69.0	1.6×10^{-2}	7.2×10^{-3}	1.1 ms		≈100		1.1×10^{-3}	[7]
^{283}Cn	9.67	9.63 s	46.5	53.5	2.1×10^{1}	1.8×10^{1}	3.81 s	94	6	4.1	6.3×10^{1}	[10]
^{284}Cn	9.46*	178 ms	0.6	99.4	3.0×10^{1}	1.8×10^{-1}	121 ms	2	98	6.0	1.2×10^{-1}	[20]
^{282}Nh	10.78	206 ms	98.6	1.4	2.1×10^{-1}	1.5×10^{1}	61 ms	100		6.1×10^{-2}		[11]
^{283}Nh	10.36*	677 ms	69.6	30.4	9.7×10^{-1}	2.2	123 ms	100		1.2×10^{-1}		[11]
^{284}Nh	10.28	3.61 s	95.4	4.6	3.8	7.9×10^{1}	0.90 s	100		9.0×10^{-1}		[11]
^{285}Nh	10.01	4.21 s	52.0	48.0	8.1	8.8	2.1 s	82	18	2.6	1.2×10^{1}	[11]
^{286}Nh	9.79	1.10 min	84.1	15.9	7.9×10^{1}	4.2×10^{2}	12 s	100		1.2×10^{1}		[7]
^{284}Fl	10.76*	3.09 ms	6.7	93.3	4.6×10^{-2}	3.3×10^{-3}	2 ms	≤20	100	≥8.0×10^{-3}	2.0×10^{-3}	[23]
^{285}Fl	10.56	313 ms	78.7	21.3	4.0×10^{-1}	1.5	210 ms	≈100	<20	2.1×10^{-1}	>1.0	[7]
^{286}Fl	10.34	14.8 ms	2.7	97.3	5.4×10^{-1}	1.5×10^{-2}	105 ms	55	45	1.9×10^{-1}	2.3×10^{-1}	[10]
^{287}Fl	10.16	2.60 s	59.6	40.4	4.4	6.4	510 ms	≈100		5.1×10^{-1}		[7]
^{288}Fl	10.08	48.5 ms	1.8	98.2	2.6	4.9×10^{-2}	653 ms	≈100		6.5×10^{-1}		[7]
^{286}Mc	10.86	552 ms	95.6	4.4	5.8×10^{-1}	1.2×10^{1}	20 ms	100		2.0×10^{-2}		[11]
^{287}Mc	10.76	293 ms	69.7	30.3	4.2×10^{-1}	9.7×10^{-1}	60 ms	100		6.0×10^{-2}		[7]
^{288}Mc	10.65	1.81 s	95.0	5.0	1.9	3.6×10^{1}	177 ms	100		1.8×10^{-1}		[7]
^{289}Mc	10.49	1.23 s	61.7	38.3	2.0	3.2	410 ms	100		4.1×10^{-1}		[7]
^{290}Mc	10.41	7.24 s	93.6	6.4	7.7	1.1×10^{2}	840 ms	100		8.4×10^{-1}		[7]
^{288}Lv	11.24*	1.11 ms	8.0	92.0	1.4×10^{-2}	1.2×10^{-3}	2.0 ms	100		2.0×10^{-3}		[70]
^{289}Lv	11.06*	85.0 ms	83.5	16.5	1.0×10^{-1}	5.2×10^{-1}	12 ms	100		1.2×10^{-2}		[69]
^{290}Lv	11.00	3.55 ms	6.8	93.2	5.2×10^{-2}	3.8×10^{-3}	9 ms	≈100		9.0×10^{-3}		[7]
^{291}Lv	10.89	219 ms	84.2	15.8	2.6×10^{-1}	1.4	26 ms	≈100		2.6×10^{-2}		[7]
^{292}Lv	10.79	10.4 ms	6.2	93.8	1.7×10^{-1}	1.1×10^{-2}	16 ms	≈100		1.6×10^{-2}		[7]
^{293}Ts	11.32	70.4 ms	87.5	12.5	8.0×10^{-2}	5.6×10^{-1}	25 ms	100		2.5×10^{-2}		[7]
^{294}Ts	11.18	406 ms	98.2	1.8	4.1×10^{-1}	2.3×10^{1}	70 ms	100		7.0×10^{-2}		[7]
^{294}Og	11.87	479 μs	22.1	77.9	2.2×10^{-3}	6.1×10^{-4}	0.7 ms	≈100		7.0×10^{-4}		[7]
^{295}Og	*11.93*	4.22 ms	97.3	2.7	4.3×10^{-3}	1.6×10^{-1}	680 ms	≈100		6.8×10^{-1}		[7]

CPC Accepted

Refs. [39, 84] predict competition, whereas Refs. [37, 38] favour α decay. In particular, for ^{290}Lv, Refs. [39] and [84] give $T_{1/2}^{\rm SF}=13$ ms and 10 ms, respectively, which are comparable to the $T_{1/2}^{\alpha}=52$ ms calculated from $Q_\alpha^{\rm exp}$ using Eq. (1) and thus lead to the same competition between the two modes. In contrast, Refs. [37] and [38] give $T_{1/2}^{\rm SF}=12$ min and 3 y, respectively, and therefore favour α decay.

For ^{272}Hs, ^{283}Cn, and ^{294}Og, competition between α decay and SF is predicted. For ^{272}Hs and ^{294}Og, only α decay has been observed, whereas for ^{283}Cn, the available experimental data on both modes show α-decay dominance. For ^{272}Hs, Ref. [39] gives $T_{1/2}^{\rm SF}=66$ ms, which is comparable to $T_{1/2}^{\alpha}\left(Q_\alpha^{\rm exp}\right)=170$ ms and therefore also indicates competition, whereas Ref. [38] gives $T_{1/2}^{\rm SF}=9$ days, which strongly favours α decay. For ^{294}Og, all four

microscopic models [37−39, 84] predict α-decay dominance when compared with the corresponding $T^{\alpha}_{1/2}\left(Q^{\rm exp}_{\alpha}\right)$ value; in particular, Ref. [84] gives $T^{\rm SF}_{1/2}=3.2\times10^{-1}$ s, which is consistent with the experimentally observed α decay. For ^{283}Cn, no microscopic calculations of $T^{\rm SF}_{1/2}$ have been reported. Nevertheless, the experimental values of the two half-lives differ by a factor of less than 16, so this observation does not contradict the competition predicted by the empirical formulas.

The spread among the microscopic predictions of $T^{\rm SF}_{1/2}$ is substantial and exceeds ten orders of magnitude for several nuclei. For example, for ^{288}Fl, the values of $T^{\rm SF}_{1/2}$ are 8.7×10^{-6} s [39], 2.4×10^{6} s [38], 2.1×10^{3} s [36], and 1.0×10^{-2} s [84], spanning about twelve orders of magnitude. This spread makes it difficult to draw unambiguous conclusions about the dominant decay mode from any single microscopic prediction. Furthermore, the discrepancies in the predicted dominant decay modes may reflect the sensitivity of $T^{\alpha}_{1/2}$ and $T^{\rm SF}_{1/2}$, calculated with Eqs. (1) and (2), respectively, to Q_{α} and especially to variations in the predicted Q_{α} values among different mass models.

To assess the robustness of the predicted dominant decay modes against variations in the input Q_{α} values, we performed a sensitivity analysis by varying Q_{α} by $\pm\delta^{Q_{\alpha}}$. For nuclei with an experimental $Q^{\rm exp}_{\alpha}$ value, the calculations were performed using $Q^{\rm exp}_{\alpha}$ and $Q^{\rm exp}_{\alpha}\pm Q^{\rm err}_{\alpha}$, where $Q^{\rm err}_{\alpha}$ is the experimental uncertainty; thus, $\delta^{Q_{\alpha}}=Q^{\rm err}_{\alpha}$. Both $Q^{\rm exp}_{\alpha}$ and $Q^{\rm err}_{\alpha}$ were taken from Ref. [62]. For the remaining nuclei, for which only the theoretical $Q^{\rm th}_{\alpha}$ value from Ref. [63] is available, $Q^{\rm th}_{\alpha}$ was varied by $\pm\delta^{Q_{\alpha}}_{\rm rms}=\pm315$ keV, so that $\delta^{Q_{\alpha}}=\delta^{Q_{\alpha}}_{\rm rms}$. The competition regime between α decay and SF was defined by $\left|\log_{10}\left(T^{\alpha}_{1/2}/T^{\rm SF}_{1/2}\right)\right|\le1$. The complete set of predictions for all 108 nuclei in the region $103\le Z\le120$ and $55\le N-Z\le60$ is given in Table 2 in Appendix B.

Among the 108 nuclei considered, 85 (78.7%) retain their predicted dominant decay mode under the Q_{α} variation, whereas 23 (21.3%) change it. In all cases, the change occurs at only one of the two limits, while the other limit preserves the same mode as the central value. Moreover, the transition always occurs between a single dominant mode and the competition regime, and never directly between α decay and SF.

The 23 nuclei for which the prediction changes can be divided into four groups. For 13 of them, the change occurs when Q_{α} is increased, $Q_{\alpha}+\delta^{Q_{\alpha}}$. In 7 of these cases, ^{271}Sg, ^{270}Bh, ^{271,273}Hs, ^{282}Rg, ^{281}Cn, and ^{300}120, the competition regime is replaced by α-decay dominance. In the remaining 6 cases, ^{261,262,266}Lr, ^{267}Rf, ^{269}Db, and ^{276}Hs, SF dominance is replaced by competition. For the other 10 nuclei, the change occurs when Q_{α} is decreased, $Q_{\alpha}-\delta^{Q_{\alpha}}$. In 7 of these cases, ^{274}Bh, ^{281}Rg, ^{287}Lv, ^{289,291}Ts, ^{293}Og, and ^{293}119, α-decay dominance is replaced by competition. In the remaining 3 cases, ^{268}Db, ^{274}Hs, and ^{280}Ds, the competition regime is replaced by SF dominance.

The predicted modes were also compared with available experimental data. For 13 of the 23 nuclei for which the prediction changes upon Q_{α} variation, experimental information on at least one decay mode is available. In 5 cases (^{270}Bh, ^{273}Hs, ^{280}Ds, and ^{281,282}Rg), varying Q_{α} brings the predicted mode into agreement with the experimental observation, whereas the central prediction disagrees. For example, for ^{281}Rg, the central Q_{α} value yields α dominance with $T^{\alpha}_{1/2}=0.22$ s and $T^{\rm SF}_{1/2}=4.2$ s, whereas the experimental data indicate competition between the two modes. Lowering Q_{α} by $\delta^{Q_{\alpha}}_{\rm rms}$ gives $T^{\alpha}_{1/2}=1.4$ s and $T^{\rm SF}_{1/2}=8.1$ s, placing the prediction within the competition regime and in agreement with experiment. For ^{282}Rg, the central prediction gives competition with $T^{\alpha}_{1/2}=1.9$ min and $T^{\rm SF}_{1/2}=13$ min, while only α decay has been observed experimentally. Increasing Q_{α} yields $T^{\alpha}_{1/2}=15$ s and $T^{\rm SF}_{1/2}=6.7$ min, shifting the prediction to α dominance and restoring agreement with experiment. Conversely, for ^{280}Ds, the central prediction gives competition with $T^{\alpha}_{1/2}=348$ ms and $T^{\rm SF}_{1/2}=70$ s, whereas SF is observed experimentally. Decreasing Q_{α} yields $T^{\alpha}_{1/2}=2.5$ s and $T^{\rm SF}_{1/2}=0.14$ s, resulting in SF dominance and a correct prediction.

The sensitivity analysis shows that predictions for nuclei in the competition regime are inherently sensitive to Q_{α} variations and should therefore be treated with caution.

The few remaining mismatches highlight the sensitivity of decay competition to fine structural details of the nucleus and indicate the limitations of the empirical formulas in regimes where the two decay modes are in close competition. Nevertheless, the overall agreement for the vast majority of cases supports the reliability of the formulas for predicting the dominant decay mode in yet unexplored nuclei.

III. Discussion of α-decay chains

The total half-life of each nucleus, considering only α decay and SF, is calculated as

$$T_{1/2}=\left(\frac{1}{T^{\alpha}_{1/2}}+\frac{1}{T^{\rm SF}_{1/2}}\right)^{-1}, \tag{3}$$

where the branching ratios are defined as $b_{\alpha}=T_{1/2}/T^{\alpha}_{1/2}$ and $b_{\rm SF}=T_{1/2}/T^{\rm SF}_{1/2}$, so that $b_{\alpha}+b_{\rm SF}=1$. The quoted branching ratios are normalized within the two-channel (α decay and SF) approximation.

The partial half-lives $T^{\alpha}_{1/2}$ and $T^{\rm SF}_{1/2}$ are taken from three sources in order of priority. Direct experimental half-lives from Refs. [7, 29] are used whenever available. If no direct experimental half-life is available but an ex-

CPC Accepted

Table 2. Calculated α-decay and SF half-lives, together with the resulting dominant decay modes, for 108 nuclei with $103 \le Z \le 120$ and $55 \le N-Z \le 60$. The second column lists experimental $Q_\alpha^{\rm exp}$ values from Ref. [62] with their errors $Q_\alpha^{\rm err}$, while theoretical $Q_\alpha^{\rm th}$ values from Ref. [63] are shown in italic. For nuclei with an experimental $Q_\alpha^{\rm exp}$ value, the calculations are performed using $Q_\alpha^{\rm exp}$ and $Q_\alpha^{\rm exp} \pm Q_\alpha^{\rm err}$, so that $\delta^{Q_\alpha} = Q_\alpha^{\rm err}$. Otherwise, the theoretical $Q_\alpha^{\rm th}$ value from Ref. [63] is varied by $\pm\delta_{\rm rms}^{Q_\alpha}$, so that $\delta^{Q_\alpha} = \delta_{\rm rms}^{Q_\alpha} = 315$ keV. All Q_α values are given in MeV. For each Q_α value, $T_{1/2}^{\alpha}$ and $T_{1/2}^{\rm SF}$ are calculated from Eq. (1) and Eq. (2), respectively. All half-lives are given in seconds. The dominant decay mode is classified as α if $\log_{10}(T_{1/2}^{\alpha}/T_{1/2}^{\rm SF}) < -1$, SF if $\log_{10}(T_{1/2}^{\alpha}/T_{1/2}^{\rm SF}) > +1$, and competition otherwise, i.e., when the two half-lives agree within one order of magnitude. In the competition regime, the first symbol indicates the formally dominant mode. The last column indicates whether the dominant decay mode changes upon variation of Q_α. A blank cell indicates no change, whereas $+\delta^{Q_\alpha}$ or $-\delta^{Q_\alpha}$ indicates the cases in which the mode differs from the prediction obtained with the central Q_α value.

Nuclide	Q_α	Q_α			$Q_\alpha + \delta^{Q_\alpha}$			$Q_\alpha - \delta^{Q_\alpha}$			Mode shift
		$T_{1/2}^{\alpha}$	$T_{1/2}^{\rm SF}$	Mode	$T_{1/2}^{\alpha}$	$T_{1/2}^{\rm SF}$	Mode	$T_{1/2}^{\alpha}$	$T_{1/2}^{\rm SF}$	Mode	
^{261}Lr	*7.870*	8.8×10^{3}	2.2×10^{2}	SF	7.2×10^{2}	1.1×10^{2}	SF/α	1.3×10^{5}	4.2×10^{2}	SF	$+\delta^{Q_\alpha}$
^{262}Lr	*7.410*	1.1×10^{6}	1.7×10^{4}	SF	7.1×10^{4}	8.8×10^{3}	SF/α	2.0×10^{7}	3.3×10^{4}	SF	$+\delta^{Q_\alpha}$
^{263}Lr	*7.170*	4.1×10^{6}	1.8×10^{3}	SF	2.3×10^{5}	9.2×10^{2}	SF	8.8×10^{7}	3.4×10^{3}	SF	
^{264}Lr	*6.560*	4.6×10^{9}	1.9×10^{5}	SF	1.7×10^{8}	9.9×10^{4}	SF	1.5×10^{11}	3.7×10^{5}	SF	
^{265}Lr	*6.520*	2.9×10^{9}	1.3×10^{4}	SF	1.1×10^{8}	6.8×10^{3}	SF	1.0×10^{11}	2.5×10^{4}	SF	
^{266}Lr	*7.420*	1.0×10^{6}	6.0×10^{4}	SF	6.5×10^{4}	3.1×10^{4}	SF/α	1.8×10^{7}	1.2×10^{5}	SF	$+\delta^{Q_\alpha}$
^{263}Rf	*7.850*	1.6×10^{4}	2.3×10^{2}	SF	1.3×10^{3}	1.2×10^{2}	SF	2.3×10^{5}	4.4×10^{2}	SF	
^{264}Rf	*7.650*	3.1×10^{4}	2.2	SF	2.2×10^{3}	1.2	SF	5.1×10^{5}	4.3	SF	
^{265}Rf	*7.090*	1.4×10^{7}	2.1×10^{3}	SF	7.4×10^{5}	1.1×10^{3}	SF	3.3×10^{8}	4.1×10^{3}	SF	
^{266}Rf	*7.050*	7.6×10^{6}	1.5×10^{1}	SF	3.9×10^{5}	7.7	SF	1.8×10^{8}	2.9×10^{1}	SF	
^{267}Rf	*7.850*	1.6×10^{4}	8.1×10^{2}	SF	1.3×10^{3}	4.2×10^{2}	SF/α	2.3×10^{5}	1.6×10^{3}	SF	$+\delta^{Q_\alpha}$
^{268}Rf	*7.760*	1.2×10^{4}	6.3	SF	9.3×10^{2}	3.3	SF	1.9×10^{5}	1.2×10^{1}	SF	
^{265}Db	*7.800*	9.4×10^{4}	2.5×10^{2}	SF	7.1×10^{3}	1.3×10^{2}	SF	1.5×10^{6}	4.9×10^{2}	SF	
^{266}Db	*7.330*	1.4×10^{7}	2.0×10^{4}	SF	8.5×10^{5}	1.0×10^{4}	SF	3.0×10^{8}	3.9×10^{4}	SF	
^{267}Db	*7.320*	6.6×10^{6}	1.3×10^{3}	SF	3.9×10^{5}	6.7×10^{2}	SF	1.3×10^{8}	2.5×10^{3}	SF	
^{268}Db	*8.170*	1.1×10^{4}	6.6×10^{3}	SF/α	9.9×10^{2}	3.4×10^{3}	α/SF	1.4×10^{5}	1.3×10^{4}	SF	$-\delta^{Q_\alpha}$
^{269}Db	*8.100*	8.0×10^{3}	4.8×10^{2}	SF	7.0×10^{2}	2.5×10^{2}	SF/α	1.1×10^{5}	9.3×10^{2}	SF	$+\delta^{Q_\alpha}$
^{270}Db	*8.150*	1.3×10^{4}	1.3×10^{4}	SF/α	1.2×10^{3}	6.7×10^{3}	α/SF	1.7×10^{5}	2.5×10^{4}	SF/α	
^{267}Sg	8.400 ± 0.050	1.1×10^{3}	7.2×10^{1}	SF	7.8×10^{2}	6.5×10^{1}	SF	1.7×10^{3}	8.0×10^{1}	SF	
^{268}Sg	*7.890*	2.5×10^{4}	1.4	SF	1.9×10^{3}	7.0×10^{-1}	SF	3.7×10^{5}	2.6	SF	
^{269}Sg	8.550 ± 0.013	3.7×10^{2}	9.9×10^{1}	SF/α	3.4×10^{2}	9.6×10^{1}	SF/α	4.1×10^{2}	1.0×10^{2}	SF/α	
^{270}Sg	*8.740*	3.4×10^{1}	4.3×10^{-1}	SF	3.7	2.2×10^{-1}	SF	3.5×10^{2}	8.3×10^{-1}	SF	
^{271}Sg	*8.840*	4.5×10^{1}	1.0×10^{2}	α/SF	5.2	5.3×10^{1}	α	4.5×10^{2}	2.0×10^{2}	SF/α	$+\delta^{Q_\alpha}$
^{272}Sg	*8.500*	2.0×10^{2}	1.3	SF	2.0×10^{1}	6.9×10^{-1}	SF	2.2×10^{3}	2.6	SF	
^{269}Bh	*8.260*	1.3×10^{4}	9.6×10^{1}	SF	1.1×10^{3}	5.0×10^{1}	SF	1.6×10^{5}	1.9×10^{2}	SF	
^{270}Bh	9.064 ± 0.095	8.3×10^{1}	5.3×10^{2}	α/SF	4.4×10^{1}	4.4×10^{2}	α	1.6×10^{2}	6.5×10^{2}	α/SF	$+\delta^{Q_\alpha}$
^{271}Bh	9.420 ± 0.086	3.2	1.6×10^{1}	α/SF	1.9	1.3×10^{1}	α/SF	5.7	1.9×10^{1}	α/SF	
^{272}Bh	9.303 ± 0.054	1.7×10^{1}	6.1×10^{2}	α	1.2×10^{1}	5.5×10^{2}	α	2.4×10^{1}	6.8×10^{2}	α	
^{273}Bh	*8.830*	1.8×10^{2}	1.0×10^{2}	SF/α	2.0×10^{1}	5.4×10^{1}	α/SF	1.8×10^{3}	2.0×10^{2}	SF/α	
^{274}Bh	8.940 ± 0.060	2.0×10^{2}	2.5×10^{3}	α	1.3×10^{2}	2.2×10^{3}	α	3.0×10^{2}	2.8×10^{3}	α/SF	$-\delta^{Q_\alpha}$
^{271}Hs	9.480 ± 0.020	3.0	7.5	α/SF	2.7	7.2	α/SF	3.4	7.8	α/SF	
^{272}Hs	9.772 ± 0.021	1.7×10^{-1}	2.6×10^{-2}	SF/α	1.5×10^{-1}	2.5×10^{-2}	SF/α	2.0×10^{-1}	2.7×10^{-2}	SF/α	

CPC Accepted

Table 2-continued from previous page

Nuclide	Q_α	Q_α			$Q_\alpha+\delta^{Q_\alpha}$			$Q_\alpha-\delta^{Q_\alpha}$			Mode shift
		$T^{\alpha}_{1/2}$	$T^{\mathrm{SF}}_{1/2}$	Mode	$T^{\alpha}_{1/2}$	$T^{\mathrm{SF}}_{1/2}$	Mode	$T^{\alpha}_{1/2}$	$T^{\mathrm{SF}}_{1/2}$	Mode	
^{273}Hs	9.650 ± 0.064	1.0	9.9	α/SF	6.9×10^{-1}	8.6	α	1.5	1.1×10^{1}	α/SF	$+\delta^{Q_\alpha}$
^{274}Hs	*9.560*	6.6×10^{-1}	7.7×10^{-2}	SF/α	9.3×10^{-2}	4.0×10^{-2}	SF/α	5.2	1.5×10^{-1}	SF	$-\delta^{Q_\alpha}$
^{275}Hs	9.450 ± 0.054	3.7	2.8×10^{1}	α/SF	2.6	2.5×10^{1}	α/SF	5.2	3.2×10^{1}	α/SF	
^{276}Hs	*9.190*	7.5	3.2×10^{-1}	SF	9.4×10^{-1}	1.6×10^{-1}	SF/α	6.7×10^{1}	6.1×10^{-1}	SF	$+\delta^{Q_\alpha}$
^{273}Mt	*11.110*	8.6×10^{-4}	2.5×10^{-1}	α	1.8×10^{-4}	1.3×10^{-1}	α	4.5×10^{-3}	4.8×10^{-1}	α	
^{274}Mt	*11.010*	3.5×10^{-3}	9.1	α	7.0×10^{-4}	4.7	α	1.9×10^{-2}	1.8×10^{1}	α	
^{275}Mt	10.483 ± 0.051	2.5×10^{-2}	1.7	α	1.9×10^{-2}	1.6	α	3.3×10^{-2}	1.9	α	
^{276}Mt	10.100 ± 0.010	5.5×10^{-1}	1.2×10^{2}	α	5.1×10^{-1}	1.1×10^{2}	α	5.8×10^{-1}	1.2×10^{2}	α	
^{277}Mt	*10.130*	1.9×10^{-1}	6.8	α	3.1×10^{-2}	3.5	α	1.3	1.3×10^{1}	α	
^{278}Mt	9.580 ± 0.030	1.3×10^{1}	6.5×10^{2}	α	1.1×10^{1}	6.1×10^{2}	α	1.6×10^{1}	6.9×10^{2}	α	
^{275}Ds	11.370 ± 0.020	2.9×10^{-4}	1.4×10^{-1}	α	2.6×10^{-4}	1.4×10^{-1}	α	3.2×10^{-4}	1.5×10^{-1}	α	
^{276}Ds	10.904 ± 0.028	1.2×10^{-3}	2.4×10^{-3}	α/SF	1.0×10^{-3}	2.3×10^{-3}	α/SF	1.4×10^{-3}	2.6×10^{-3}	α/SF	
^{277}Ds	10.710 ± 0.040	9.2×10^{-3}	1.1	α	7.4×10^{-3}	9.9×10^{-1}	α	1.1×10^{-2}	1.2	α	
^{278}Ds	*10.550*	8.1×10^{-3}	9.7×10^{-3}	α/SF	1.4×10^{-3}	5.0×10^{-3}	α/SF	4.9×10^{-2}	1.9×10^{-2}	SF/α	
^{279}Ds	9.827 ± 0.015	1.6	1.3×10^{1}	α/SF	1.4	1.2×10^{1}	α/SF	1.7	1.3×10^{1}	α/SF	
^{280}Ds	*9.910*	3.5×10^{-1}	7.0×10^{-2}	SF/α	5.2×10^{-2}	3.6×10^{-2}	SF/α	2.5	1.4×10^{-1}	SF	$-\delta^{Q_\alpha}$
^{277}Rg	*11.640*	2.4×10^{-4}	8.1×10^{-2}	α	5.4×10^{-5}	4.2×10^{-2}	α	1.2×10^{-3}	1.6×10^{-1}	α	
^{278}Rg	10.846 ± 0.095	3.5×10^{-2}	1.3×10^{1}	α	2.1×10^{-2}	1.0×10^{1}	α	5.9×10^{-2}	1.6×10^{1}	α	
^{279}Rg	10.530 ± 0.168	8.3×10^{-2}	1.6	α	3.3×10^{-2}	1.1	α	2.2×10^{-1}	2.2	α	
^{280}Rg	10.149 ± 0.010	1.8	1.0×10^{2}	α	1.7	1.0×10^{2}	α	2.0	1.1×10^{2}	α	
^{281}Rg	*10.360*	2.2×10^{-1}	4.2	α	3.7×10^{-2}	2.2	α	1.4	8.2	α/SF	$-\delta^{Q_\alpha}$
^{282}Rg	*9.490*	1.2×10^{2}	7.8×10^{2}	α/SF	1.5×10^{1}	4.0×10^{2}	α	9.9×10^{2}	1.5×10^{3}	α/SF	$+\delta^{Q_\alpha}$
^{279}Cn	*11.450*	7.8×10^{-4}	1.2×10^{-1}	α	1.7×10^{-4}	6.2×10^{-2}	α	4.0×10^{-3}	2.3×10^{-1}	α	
^{280}Cn	*11.390*	3.9×10^{-4}	8.8×10^{-4}	α/SF	8.1×10^{-5}	4.6×10^{-4}	α/SF	2.0×10^{-3}	1.7×10^{-3}	SF/α	
^{281}Cn	10.418 ± 0.017	2.1×10^{-1}	2.0	α/SF	1.9×10^{-1}	1.9	α	2.3×10^{-1}	2.0	α/SF	$+\delta^{Q_\alpha}$
^{282}Cn	*10.690*	1.6×10^{-2}	7.2×10^{-3}	SF/α	2.9×10^{-3}	3.7×10^{-3}	α/SF	9.7×10^{-2}	1.4×10^{-2}	SF/α	
^{283}Cn	9.667 ± 0.015	2.1×10^{1}	1.8×10^{1}	SF/α	1.9×10^{1}	1.7×10^{1}	SF/α	2.3×10^{1}	1.9×10^{1}	SF/α	
^{284}Cn	9.460 ± 0.010	3.0×10^{1}	1.8×10^{-1}	SF	2.8×10^{1}	1.8×10^{-1}	SF	3.2×10^{1}	1.8×10^{-1}	SF	
^{281}Nh	*11.560*	1.4×10^{-3}	9.6×10^{-2}	α	3.1×10^{-4}	5.0×10^{-2}	α	7.2×10^{-3}	1.9×10^{-1}	α	
^{282}Nh	10.783 ± 0.095	2.1×10^{-1}	1.5×10^{1}	α	1.2×10^{-1}	1.2×10^{1}	α	3.6×10^{-1}	1.8×10^{1}	α	
^{283}Nh	10.360 ± 0.042	9.7×10^{-1}	2.2	α/SF	7.6×10^{-1}	2.0	α/SF	1.2	2.4	α/SF	
^{284}Nh	10.280 ± 0.038	3.8	7.9×10^{1}	α	3.0	7.3×10^{1}	α	4.8	8.6×10^{1}	α	
^{285}Nh	10.010 ± 0.040	8.1	8.8	α/SF	6.3	8.1	α/SF	1.0×10^{1}	9.5	SF/α	
^{286}Nh	9.790 ± 0.050	7.9×10^{1}	4.2×10^{2}	α/SF	5.7×10^{1}	3.7×10^{2}	α/SF	1.1×10^{2}	4.6×10^{2}	α/SF	
^{283}Fl	*11.800*	5.5×10^{-4}	5.8×10^{-2}	α	1.2×10^{-4}	3.0×10^{-2}	α	2.6×10^{-3}	1.1×10^{-1}	α	
^{284}Fl	10.760 ± 0.100	4.6×10^{-2}	3.3×10^{-3}	SF	2.7×10^{-2}	2.7×10^{-3}	SF/α	8.2×10^{-2}	4.1×10^{-3}	SF	$+\delta^{Q_\alpha}$
^{285}Fl	10.560 ± 0.071	4.0×10^{-1}	1.5	α/SF	2.6×10^{-1}	1.3	α/SF	6.0×10^{-1}	1.7	α/SF	
^{286}Fl	10.335 ± 0.010	5.4×10^{-1}	1.5×10^{-2}	SF	5.1×10^{-1}	1.5×10^{-2}	SF	5.8×10^{-1}	1.6×10^{-2}	SF	

CPC Accepted

Table 2-continued from previous page

Nuclide	Q_α	Q_α			$Q_\alpha+\delta^{Q_\alpha}$			$Q_\alpha-\delta^{Q_\alpha}$			Mode shift
		$T^{\alpha}_{1/2}$	$T^{\rm SF}_{1/2}$	Mode	$T^{\alpha}_{1/2}$	$T^{\rm SF}_{1/2}$	Mode	$T^{\alpha}_{1/2}$	$T^{\rm SF}_{1/2}$	Mode	
^{287}Fl	10.157 ± 0.010	4.4	6.4	α/SF	4.1	6.3	α/SF	4.6	6.6	α/SF	
^{288}Fl	10.076 ± 0.012	2.6	4.9×10^{-2}	SF	2.4	4.8×10^{-2}	SF	2.8	5.1×10^{-2}	SF	
^{285}Mc	*11.830*	1.5×10^{-3}	5.4×10^{-2}	α	3.3×10^{-4}	2.8×10^{-2}	α	7.2×10^{-3}	1.1×10^{-1}	α	
^{286}Mc	10.860 ± 0.020	5.8×10^{-1}	1.2×10^{1}	α	5.2×10^{-1}	1.2×10^{1}	α	6.5×10^{-1}	1.3×10^{1}	α	
^{287}Mc	10.760 ± 0.071	4.2×10^{-1}	9.7×10^{-1}	α/SF	2.8×10^{-1}	8.3×10^{-1}	α/SF	6.3×10^{-1}	1.1	α/SF	
^{288}Mc	10.650 ± 0.050	1.9	3.6×10^{1}	α	1.4	3.3×10^{1}	α	2.5	4.0×10^{1}	α	
^{289}Mc	10.490 ± 0.050	2.0	3.2	α/SF	1.5	2.9	α/SF	2.7	3.6	α/SF	
^{290}Mc	10.410 ± 0.040	7.7	1.1×10^{2}	α	6.1	1.0×10^{2}	α	9.8	1.2×10^{2}	α	
^{287}Lv	*11.570*	6.8×10^{-3}	9.4×10^{-2}	α	1.4×10^{-3}	4.8×10^{-2}	α	3.5×10^{-2}	1.8×10^{-1}	α/SF	$-\delta^{Q_\alpha}$
^{288}Lv	11.240 ± 0.015	1.4×10^{-2}	1.2×10^{-3}	SF	1.3×10^{-2}	1.2×10^{-3}	SF	1.5×10^{-2}	1.3×10^{-3}	SF	
^{289}Lv	11.059 ± 0.013	1.0×10^{-1}	5.2×10^{-1}	α/SF	9.5×10^{-2}	5.0×10^{-1}	α/SF	1.1×10^{-1}	5.3×10^{-1}	α/SF	
^{290}Lv	10.997 ± 0.058	5.2×10^{-2}	3.8×10^{-3}	SF	3.8×10^{-2}	3.4×10^{-3}	SF	7.2×10^{-2}	4.3×10^{-3}	SF	
^{291}Lv	10.890 ± 0.086	2.6×10^{-1}	1.4	α/SF	1.6×10^{-1}	1.2	α/SF	4.2×10^{-1}	1.7	α/SF	
^{292}Lv	10.791 ± 0.012	1.7×10^{-1}	1.1×10^{-2}	SF	1.5×10^{-1}	1.1×10^{-2}	SF	1.8×10^{-1}	1.1×10^{-2}	SF	
^{289}Ts	*12.080*	1.7×10^{-3}	3.2×10^{-2}	α	3.8×10^{-4}	1.7×10^{-2}	α	8.0×10^{-3}	6.2×10^{-2}	α/SF	$-\delta^{Q_\alpha}$
^{290}Ts	*11.840*	1.3×10^{-2}	1.6	α	2.9×10^{-3}	8.2×10^{-1}	α	6.6×10^{-2}	3.1	α	
^{291}Ts	*11.730*	9.6×10^{-3}	1.3×10^{-1}	α	2.0×10^{-3}	6.5×10^{-2}	α	4.9×10^{-2}	2.4×10^{-1}	α/SF	$-\delta^{Q_\alpha}$
^{292}Ts	*11.470*	8.8×10^{-2}	6.5	α	1.8×10^{-2}	3.4	α	4.7×10^{-1}	1.3×10^{1}	α	
^{293}Ts	11.320 ± 0.050	8.0×10^{-2}	5.6×10^{-1}	α/SF	6.2×10^{-2}	5.1×10^{-1}	α/SF	1.1×10^{-1}	6.3×10^{-1}	α/SF	
^{294}Ts	11.180 ± 0.040	4.1×10^{-1}	2.3×10^{1}	α	3.3×10^{-1}	2.1×10^{1}	α	5.1×10^{-1}	2.5×10^{1}	α	
^{291}Og	*12.420*	4.1×10^{-4}	1.6×10^{-2}	α	9.6×10^{-5}	8.2×10^{-3}	α	1.8×10^{-3}	3.1×10^{-2}	α	
^{292}Og	*12.280*	2.9×10^{-4}	1.4×10^{-4}	SF/α	6.7×10^{-5}	7.1×10^{-5}	α/SF	1.3×10^{-3}	2.7×10^{-4}	SF/α	
^{293}Og	*12.020*	2.8×10^{-3}	6.9×10^{-2}	α	6.1×10^{-4}	3.6×10^{-2}	α	1.3×10^{-2}	1.3×10^{-1}	α/SF	$-\delta^{Q_\alpha}$
^{294}Og	11.867 ± 0.031	2.2×10^{-3}	6.1×10^{-4}	SF/α	1.9×10^{-3}	5.8×10^{-4}	SF/α	2.5×10^{-3}	6.6×10^{-4}	SF/α	
^{295}Og	*11.930*	4.3×10^{-3}	1.6×10^{-1}	α	9.4×10^{-4}	8.1×10^{-2}	α	2.1×10^{-2}	3.0×10^{-1}	α	
^{296}Og	*11.920*	1.7×10^{-3}	1.0×10^{-3}	SF/α	3.6×10^{-4}	5.4×10^{-4}	α/SF	8.2×10^{-3}	2.0×10^{-3}	SF/α	
^{293}119	*12.590*	5.7×10^{-4}	1.1×10^{-2}	α	1.4×10^{-4}	5.7×10^{-3}	α	2.5×10^{-3}	2.1×10^{-2}	α/SF	$-\delta^{Q_\alpha}$
^{294}119	*12.410*	3.2×10^{-3}	4.8×10^{-1}	α	7.4×10^{-4}	2.5×10^{-1}	α	1.5×10^{-2}	9.3×10^{-1}	α	
^{295}119	*12.510*	8.3×10^{-4}	2.5×10^{-2}	α	2.0×10^{-4}	1.3×10^{-2}	α	3.7×10^{-3}	4.8×10^{-2}	α	
^{296}119	*12.750*	6.6×10^{-4}	4.5×10^{-1}	α	1.6×10^{-4}	2.3×10^{-1}	α	2.8×10^{-3}	8.7×10^{-1}	α	
^{297}119	*12.650*	4.3×10^{-4}	3.5×10^{-2}	α	1.1×10^{-4}	1.8×10^{-2}	α	1.9×10^{-3}	6.7×10^{-2}	α	
^{298}119	*13.160*	1.1×10^{-4}	3.6×10^{-1}	α	2.8×10^{-5}	1.8×10^{-1}	α	4.3×10^{-4}	6.9×10^{-1}	α	
^{295}120	*13.120*	6.3×10^{-5}	3.6×10^{-3}	α	1.6×10^{-5}	1.9×10^{-3}	α	2.6×10^{-4}	7.1×10^{-3}	α	
^{296}120	*13.240*	1.4×10^{-5}	1.8×10^{-5}	α/SF	3.6×10^{-6}	9.5×10^{-6}	α/SF	5.4×10^{-5}	3.6×10^{-5}	SF/α	
^{297}120	*13.300*	2.9×10^{-5}	4.7×10^{-3}	α	7.6×10^{-6}	2.4×10^{-3}	α	1.1×10^{-4}	9.1×10^{-3}	α	
^{298}120	*13.140*	2.1×10^{-5}	4.3×10^{-5}	α/SF	5.4×10^{-6}	2.2×10^{-5}	α/SF	8.5×10^{-5}	8.3×10^{-5}	SF/α	
^{299}120	*13.550*	1.0×10^{-5}	5.3×10^{-3}	α	2.8×10^{-6}	2.7×10^{-3}	α	3.8×10^{-5}	1.0×10^{-2}	α	
^{300}120	*13.350*	8.5×10^{-6}	5.2×10^{-5}	α/SF	2.3×10^{-6}	2.7×10^{-5}	α	3.3×10^{-5}	1.0×10^{-4}	α/SF	$+\delta^{Q_\alpha}$

CPC Accepted

perimental Q_α value is known from Ref. [62], the partial half-lives are calculated using Eq. (1) and Eq. (2). In the absence of both direct experimental half-lives and experimental Q_α values, the Q_α values predicted by the macroscopic–microscopic model of Ref. [63] are employed.

The results are summarized in Figs. 4 and 5. Each figure presents the complete decay chains for a given element and shows, for each nucleus, the total half-life, the branching ratios $b_{\rm SF}$ and b_α (in %), and the Q_α value of the parent nucleus. A detailed comparison of calculated and experimental half-lives for all nuclei with available data is given in Table 1 in Appendix A.

To systematically assess the competition between the two decay modes, we classify each nucleus according to the relative magnitudes of its partial half-lives. When the two half-lives differ by no more than one order of magnitude, i.e., $\left|\log_{10}\left(T^{\alpha}_{1/2}/T^{\rm SF}_{1/2}\right)\right| \le 1$, the nucleus is regarded as exhibiting strong competition between the two decay modes. Otherwise, if $T^{\alpha}_{1/2} < T^{\rm SF}_{1/2}$, α decay is considered to be the dominant mode, whereas if $T^{\alpha}_{1/2} > T^{\rm SF}_{1/2}$, SF is considered dominant.

We now discuss each chain individually, focusing on the competition between α decay and SF and on the prospects for experimental observation of the isotopes of elements 119 and 120 through their α-decay chains.

A. Promising chains for observation

The most favorable cases for experimental identification are those in which α decay remains the dominant mode over many consecutive steps, producing extended correlated sequences that terminate in SF. Among the isotopes of elements 119 and 120 considered here, this behavior is found in the chains starting from ^{293,294,296}119 and ^{295}120. Here and below, the number of α decays in a

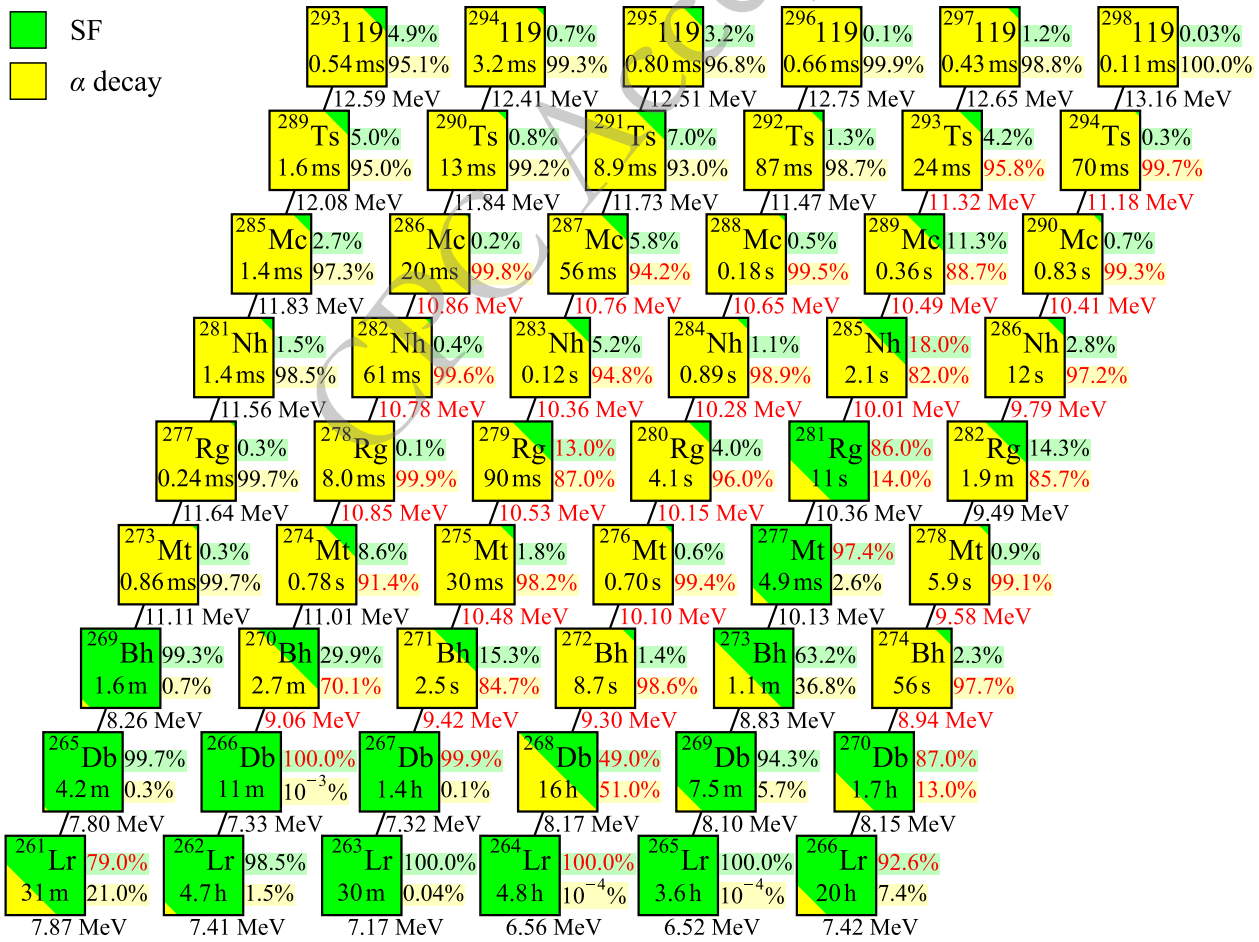


Fig. 4. (color online) α-decay chains of $Z = 119$ isotopes with mass numbers $A = 293$–298. Each cell lists the nuclear symbol and the total half-life, taking into account competition between α decay (yellow) and SF (green). The SF and α-decay branching ratios, $b_{\rm SF}$ and b_α, respectively (in %), are given to the right of each cell ($b_\alpha + b_{\rm SF} = 100\%$); the upper value is $b_{\rm SF}$, and the lower value is b_α. Branching ratios shown in red indicate that the corresponding partial half-life was taken from experimental data [7, 10−13, 20, 29]; those shown in black indicate that the partial half-lives for α decay and SF were calculated using Eq. (1) and Eq. (2), respectively. The Q_α value for each parent nucleus is shown below the cell. Red Q_α values are experimental [62], whereas black values are theoretical values obtained from Ref. [63].

CPC Accepted

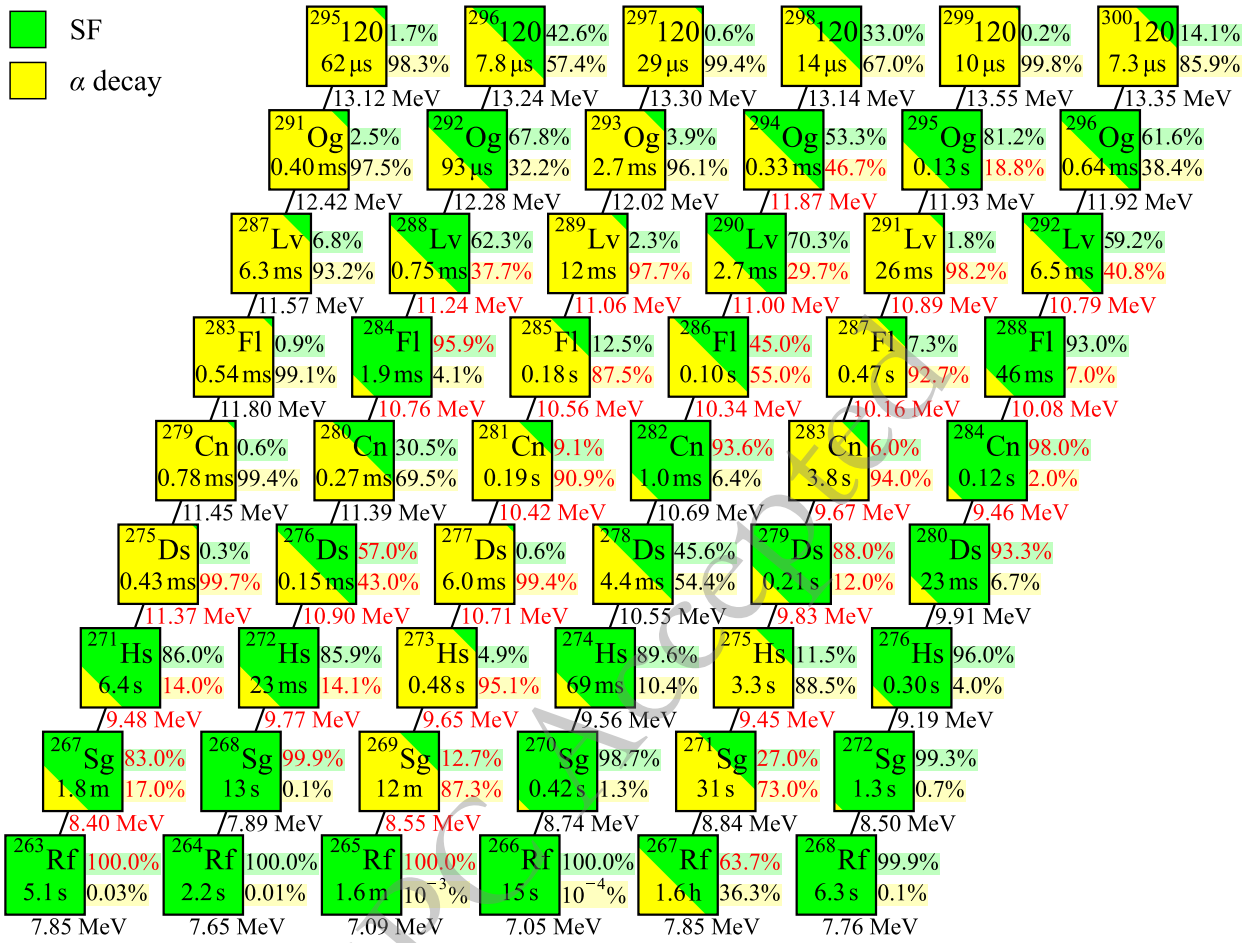


Fig. 5. (color online) Same as Fig. 4, but for the α-decay chains of $Z = 120$ isotopes with mass numbers $A = 295$–300.

chain is defined as the number of consecutive α-emitting steps up to the first nucleus that undergoes SF.

Chain starting from ^{293}119 *($N-Z=55$).* This chain provides six consecutive α decays, from ^{293}119 down to ^{273}Mt. Throughout this sequence, α decay remains clearly dominant. The transition to SF dominance occurs at ^{269}Bh, where the chain terminates. The half-lives along the α-dominated part of the chain are in the submillisecond-to-millisecond range. This chain is among the most promising candidates for experimental identification.

Chain starting from ^{294}119 *($N-Z=56$).* This chain yields seven α decays, from ^{294}119 down to ^{270}Bh. The dominance of α decay is clear from ^{294}119 through ^{274}Mt. At ^{270}Bh, competition between the two modes becomes apparent, although α decay still dominates. SF becomes dominant at ^{266}Db. Our predictions for the nuclei from ^{286}Mc onward are consistent with experimental data, which show only α decays down to ^{266}Db.

Chain starting from ^{296}119 *($N-Z=58$).* This chain provides seven α decays before SF terminates the sequence at ^{264}Lr. The dominance of α decay is clear from ^{296}119 through ^{272}Bh. At ^{268}Db, our calculations predict strong competition between the two modes, and the experimental data confirm this competition.

Chain starting from ^{295}120 *($N-Z=55$).* This chain provides six consecutive α decays, from ^{295}120 down to ^{271}Hs. Throughout this sequence, α decay remains clearly dominant. At ^{267}Sg, competition between the two modes emerges, and the chain terminates at ^{263}Rf. Our predictions for the lower part of the chain are consistent with experimental data.

B. Chains with strong competition between α decay and SF

The chains discussed in this section contain one or more nuclei exhibiting strong competition according to the above criterion, although smaller but non-negligible SF branches may occur at other steps. Although these chains may still be observable as α emitters, the presence of SF branches could affect the decay pattern or shorten the observed sequence in some cases. Such behavior is found in the chains starting from ^{295,297,298}119 and ^{297,299}120.

Chain starting from ^{295}119 *($N-Z=57$).* The dominant decay sequence contains seven consecutive α decay

Chinese Physics C

steps, from ^{295}119 down to ^{271}Bh. A noticeable SF admixture appears at ^{283}Nh and remains appreciable at ^{279}Rg. For ^{287}Mc, the experimental α-decay half-life is significantly shorter than our prediction, although α decay remains the observed mode. The chain can terminate by SF at ^{267}Db.

Chain starting from ^{297}119 *($N-Z=59$).* This chain exhibits competition between α decay and SF from the initial steps. A notable discrepancy with experiment appears at ^{281}Rg: while our calculations predict α-decay dominance with a significant SF admixture, the experimental data indicate SF as the dominant mode. An even larger discrepancy is observed at ^{277}Mt, where the experimental SF half-life is three orders of magnitude shorter than our prediction. The chain terminates at ^{265}Lr in our calculations, although the experimental observation of SF only for ^{277}Mt indicates a possible earlier termination.

Chain starting from ^{298}119 *($N-Z=60$).* Starting from ^{298}119, the chain proceeds through seven consecutive α decays down to ^{274}Bh. A noticeable SF admixture appears at ^{282}Rg and becomes strong at ^{270}Db, where the two decay modes compete. Experimental data for ^{270}Db indicate SF dominance, consistent with our predictions. The chain can terminate at ^{266}Lr.

Chain starting from ^{297}120 *($N-Z=57$).* The chain beginning at ^{297}120 undergoes seven consecutive α decays down to ^{273}Hs before SF terminates the sequence at ^{269}Sg. The dominance of α decay is clear in the initial steps. Competition becomes noticeable starting from ^{285}Fl and persists through ^{273}Hs, apart from a return to α-decay dominance at ^{277}Ds. At ^{269}Sg, our calculations predict competition between the two modes, whereas only α decay has been observed experimentally, indicating a possible overestimation of the SF branch in this nucleus.

Chain starting from ^{299}120 *($N-Z=59$).* Among the $Z=120$ isotopes, the chain starting from ^{299}120 is the longest α-dominated chain, with seven consecutive α decays. Strong competition appears already at the second decay step, at ^{295}Og, and persists throughout the chain. Notably, at ^{279}Ds, our calculations predict α-decay dominance, whereas experimental data indicate strong competition with SF. The chain continues beyond ^{267}Rf in our calculations, although the calculated SF branch becomes increasingly important.

C. Chains unfavorable for identification

For some isotopes, SF becomes the dominant decay mode at an early stage in the chain, preventing the observation of extended α-decay sequences. Among the isotopes of element 120, this behavior is found in the chains starting from ^{296,298,300}120.

Chain starting from ^{296}120 *($N-Z=56$).* This chain exhibits strong competition between α decay and SF from the first step, beginning with ^{296}120, and this competition persists throughout the chain. For ^{276}Ds, the experimentally observed competition between the two modes is consistent with our predictions. At ^{272}Hs, however, only α decay has been observed experimentally, whereas our calculations indicate a significant SF component. The chain terminates by SF at ^{268}Sg, in agreement with experiment.

Chain starting from ^{298}120 *($N-Z=58$).* This chain is characterized by strong competition already at ^{298}120, and the two modes remain competitive throughout most of the chain. For ^{294}Og and ^{290}Lv, only α decay has been observed experimentally, whereas our calculations predict competition with SF. For ^{286}Fl, the experimental data confirm competition between the two decay modes.

Chain starting from ^{300}120 *($N-Z=60$).* In this chain, strong competition is already present at ^{300}120 and continues through ^{296}Og and beyond. For ^{292}Lv and ^{288}Fl, only α decay has been observed experimentally, whereas our calculations indicate strong competition with SF. For ^{284}Cn, both the experimental data and our predictions show SF dominance, with both decay modes observed. At ^{280}Ds, only SF has been observed experimentally, consistent with our calculated SF dominance. The early onset and persistence of strong competition with SF make this chain particularly unfavorable for experimental identification via α-decay chains.

IV. Conclusions

The competition between α decay and SF was analyzed along the α-decay chains of the as-yet-unsynthesized elements $Z=119$ and $Z=120$ in the mass ranges $A=293$–298 and $A=295$–300, respectively. These ranges correspond to neutron-excess values of $N-Z=55$–60, which may be accessible in fusion-evaporation reactions. The α-decay half-lives were calculated using the Viola–Seaborg formula [45] with the Parkhomenko–Sobiczewski parameterization [56], whereas the SF half-lives were obtained using our recently proposed empirical formula [58, 59]. Theoretical Q_α values were taken from the macroscopic–microscopic model of Ref. [63] when experimental values from Ref. [62] were unavailable.

The chains originating from ^{293,294,296}119 and ^{295}120 are found to be the most favorable for experimental identification, with six or more consecutive α decays expected. For the chains originating from ^{295,297,298}119 and ^{297,299}120, the presence of significant SF branches indicates a more complex decay pattern. Among the considered isotopes, the chains originating from ^{296,298,300}120 are the least favorable, with SF becoming dominant at early stages.

The present results may be of interest for ongoing experimental searches at JINR (Dubna) [8, 85, 86], LBNL (Berkeley) [87], GSI (Darmstadt) [23, 28, 88], RIKEN (Tokyo) [89], and IMP (Lanzhou) [90], all of which are currently pursuing the synthesis of elements 119 and 120

CPC Accepted

at the upper end of the nuclear chart.

ACKNOWLEDGMENTS

This work was supported by Grant No. 25-42-00018 from the Russian Science Foundation [91].

Appendix A. Calculated and experimental α-decay and SF half-lives in tabular form

Table 1 compares the calculated and experimental half-lives of 66 nuclei in the region $103 \le Z \le 118$ and $55 \le N-Z \le 60$ for which experimental data or limits are available for at least one decay mode. The total half-lives and branching ratios are obtained using Eq. (3) within the two-channel (α decay + SF) approximation.

Appendix B. Sensitivity of the predicted decay modes to the uncertainty in Q_α

Table 2 presents the calculated α-decay and SF half-lives, the resulting dominant decay modes for the three considered input Q_α values, and an indication of whether the predicted mode is robust against the Q_α uncertainty.

CPC Accepted

References

[1] Yu. Ts. Oganessian, Journal of Physics G: Nuclear and Particle Physics **34**, R165 (2007)

[2] Yu. Ts. Oganessian and V. K. Utyonkov, Nuclear Physics A **944**, 62 (2015)

[3] Yu. Ts. Oganessian and V. K. Utyonkov, Reports on Progress in Physics **78**, 036301 (2015)

[4] Yu. Ts. Oganessian, V. K. Utyonkov, S. N. Dmitriev, Yu. V. Lobanov, M. G. Itkis, A. N. Polyakov, Yu. S. Tsyganov, A. N. Mezentsev, A. V. Yeremin, A. A. Voinov, E. A. Sokol, G. G. Gulbekian, S. L. Bogomolov, S. Iliev, V. G. Subbotin, A. M. Sukhov, G. V. Buklanov, S. V. Shishkin, V. I. Chepygin, G. K. Vostokin, N. V. Aksenov, M. Hussonnois, K. Subotic, V. I. Zagrebaev, K. J. Moody, J. B. Patin, J. F. Wild, M. A. Stoyer, N. J. Stoyer, D. A. Shaughnessy, J. M. Kenneally, P. A. Wilk, R. W. Lougheed, H. W. Gäggeler, D. Schumann, H. Bruchertseifer, and R. Eichler, Phys. Rev. C **72**, 034611 (2005)

[5] S. Hofmann and G. Münzenberg, Rev. Mod. Phys. **72**, 733 (2000)

[6] K. Morita, K. Morimoto, D. Kaji, T. Akiyama, S.-i. Goto, H. Haba, E. Ideguchi, K. Katori, H. Koura, H. Kudo, T. Ohnishi, A. Ozawa, T. Suda, K. Sueki, F. Tokanai, T. Yamaguchi, A. Yoneda, and A. Yoshida, Journal of the Physical Society of Japan **76**, 043201 (2007)

[7] F. Kondev, M. Wang, W. Huang, S. Naimi, and G. Audi, Chinese Physics C **45**, 030001 (2021)

[8] Yu. Ts. Oganessian, Eur. Phys. J. A **60**, 227 (2024)

[9] Yu. Ts. Oganessian, V. K. Utyonkov, N. D. Kovrizhnykh, F. Sh. Abdullin, S. N. Dmitriev, D. Ibadullayev, M. G. Itkis, D. A. Kuznetsov, O. V. Petrushkin, A. V. Podshibiakin, A. N. Polyakov, A. G. Popeko, R. N. Sagaidak, L. Schlattauer, I. V. Shirokovski, V. D. Shubin, M. V. Shumeiko, D. I. Solovyev, Yu. S. Tsyganov, A. A. Voinov, V. G. Subbotin, A. Yu. Bodrov, A. V. Sabel'nikov, A. V. Khalkin, V. B. Zlokazov, K. P. Rykaczewski, T. T. King, J. B. Roberto, N. T. Brewer, R. K. Grzywacz, Z. G. Gan, Z. Y. Zhang, M. H. Huang, and H. B. Yang, Phys. Rev. C **106**, L031301 (2022)

[10] Yu. Ts. Oganessian, V. K. Utyonkov, D. Ibadullayev, F. Sh. Abdullin, S. N. Dmitriev, M. G. Itkis, A. V. Karpov, N. D. Kovrizhnykh, D. A. Kuznetsov, O. V. Petrushkin, A. V. Podshibiakin, A. N. Polyakov, A. G. Popeko, R. N. Sagaidak, L. Schlattauer, V. D. Shubin, M. V. Shumeiko, D. I. Solovyev, Yu. S. Tsyganov, A. A. Voinov, V. G. Subbotin, A. Yu. Bodrov, A. V. Sabel'nikov, A. Lindner, K. P. Rykaczewski, T. T. King, J. B. Roberto, N. T. Brewer, R. K. Grzywacz, Z. G. Gan, Z. Y. Zhang, M. H. Huang, and H. B. Yang, Phys. Rev. C **106**, 024612 (2022)

[11] Yu. Ts. Oganessian, V. K. Utyonkov, N. D. Kovrizhnykh, F. Sh. Abdullin, S. N. Dmitriev, A. A. Dzhioev, D. Ibadullayev, M. G. Itkis, A. V. Karpov, D. A. Kuznetsov, O. V. Petrushkin, A. V. Podshibiakin, A. N. Polyakov, A. G. Popeko, I. S. Rogov, R. N. Sagaidak, L. Schlattauer, V. D. Shubin, M. V. Shumeiko, D. I. Solovyev, Yu. S. Tsyganov, A. A. Voinov, V. G. Subbotin, A. Yu. Bodrov, A. V. Sabel'nikov, A. V. Khalkin, K. P. Rykaczewski, T. T. King, J. B. Roberto, N. T. Brewer, R. K. Grzywacz, Z. G. Gan, Z. Y. Zhang, M. H. Huang, and H. B. Yang, Phys. Rev. C **106**, 064306 (2022)

[12] Yu. Ts. Oganessian, V. K. Utyonkov, M. V. Shumeiko, F. Sh. Abdullin, S. N. Dmitriev, D. Ibadullayev, M. G. Itkis, N. D. Kovrizhnykh, D. A. Kuznetsov, O. V. Petrushkin, A. V. Podshibiakin, A. N. Polyakov, A. G. Popeko, I. S. Rogov, R. N. Sagaidak, L. Schlattauer, V. D. Shubin, D. I. Solovyev, Yu. S. Tsyganov, A. A. Voinov, V. G. Subbotin, N. S. Bublikova, M. G. Voronyuk, A. V. Sabelnikov, A. Yu. Bodrov, Z. G. Gan, Z. Y. Zhang, M. H. Huang, and H. B. Yang, Phys. Rev. C **108**, 024611 (2023)

[13] Yu. Ts. Oganessian, V. K. Utyonkov, M. V. Shumeiko, F. Sh. Abdullin, G. G. Adamian, S. N. Dmitriev, D. Ibadullayev, M. G. Itkis, N. D. Kovrizhnykh, D. A. Kuznetsov, O. V. Petrushkin, A. V. Podshibiakin, A. N. Polyakov, A. G. Popeko, I. S. Rogov, R. N. Sagaidak, L. Schlattauer, V. D. Shubin, D. I. Solovyev, Yu. S. Tsyganov, A. A. Voinov, V. G. Subbotin, N. S. Bublikova, M. G. Voronyuk, A. V. Sabelnikov, A. Yu. Bodrov, N. V. Aksenov, A. V. Khalkin, Z. G. Gan, Z. Y. Zhang, M. H. Huang, and H. B. Yang, Phys. Rev. C **109**, 054307 (2024)

[14] J. Khuyagbaatar, P. Mosat, J. Ballof, R. A. Cantemir, Ch. E. Düllmann, K. Hermainski, F. P. Heßberger, E. Jäger, B. Kindler, J. Krier, N. Kurz, S. Löchner, B. Lommel, B. Schausten, Y. Wei, P. Wieczorek, and A. Yakushev, Phys. Rev. Lett. **134**, 022501 (2025)

[15] P. Mosat, J. Khuyagbaatar, J. Ballof, R. A. Cantemir, D. Dietzel, Ch. E. Düllmann, K. Hermainski, F. P. Heßberger, E. Jäger, B. Kindler, J. Krier, N. Kurz, B. Lommel, S. Löchner, M. Maiti, T. K. Sato, B. Schausten, J. Uusitalo, P. Wieczorek, and A. Yakushev, Phys. Rev. Lett. **134**, 232501 (2025)

[16] D. Ackermann, S. Antalic, and F. P. Heßberger, Eur. Phys. J. Spec. Top. **233**, 1017 (2024)

[17] E. M. Kozulin, G. N. Knyazheva, A. V. Karpov, V. V. Saiko, A. A. Bogachev, I. M. Itkis, K. V. Novikov, I. V. Vorobiev, I. V. Pchelintsev, E. O. Savelieva, R. S. Tikhomirov, M. G. Itkis, and Yu. Ts. Oganessian, Phys. Rev. C **109**, 034616 (2024)

[18] K. Kessaci, B. J. P. Gall, O. Dorvaux, M. Forge, A. Lopez-Martens, R. Chakma, K. Hauschild, M. L. Chelnokov, V. I. Chepigin, A. V. Isaev, A. A. Kuznetsova, O. N. Malyshev, R. Mukhin, J. Piot, A. G. Popeko, Yu. A. Popov, E. A. Sokol, A. I. Svirikhin, and A. V. Yeremin, Phys. Rev. C **110**, 054310 (2024)

[19] G. Münzenberg, M. Gupta, H. M. Devaraja, Y. K. Gambhir, S. Heinz, and S. Hofmann, Eur. Phys. J. A **59**, 21 (2023)

[20] A. Såmark-Roth, D. M. Cox, D. Rudolph, L. G. Sarmiento, B. G. Carlsson, J. L. Egido, P. Golubev, J. Heery, A. Yakushev, S. Åberg, H. M. Albers, M. Albertsson, M. Block, H. Brand, T. Calverley, R. Cantemir, R. M. Clark, Ch. E. Düllmann, J. Eberth, C. Fahlander, U. Forsberg, J. M. Gates, F. Giacoppo, M. Götz, S. Götz, R.-D. Herzberg, Y. Hrabar, E. Jäger, D. Judson, J. Khuyagbaatar, B. Kindler, I. Kojouharov, J. V. Kratz, J. Krier, N. Kurz, L. Lens, J. Ljungberg, B. Lommel, J. Louko, C.-C. Meyer, A. Mistry, C. Mokry, P. Papadakis, E. Parr, J. L. Pore, I. Ragnarsson, J. Runke, M. Schädel, H. Schaffner, B. Schausten, D. A. Shaughnessy, P. Thörle-Pospiech, N. Trautmann, and J. Uusitalo, Phys. Rev. Lett. **126**, 032503 (2021)

[21] G. G. Adamian, N. V. Antonenko, A. Diaz-Torres, and S. Heinz, Eur. Phys. J. A **56**, 47 (2020)

[22] N. Jain, M. Bhuyan, P. Mohr, and R. Kumar, Nuclear Physics A **1070**, 123387 (2026)

[23] S. Hofmann, S. Heinz, R. Mann, J. Maurer, G. Münzenberg, S. Antalic, W. Barth, H. G. Burkhard, L. Dahl, K. Eberhardt, R. Grzywacz, J. H. Hamilton, R. A. Henderson, J. M. Kenneally, B. Kindler, I. Kojouharov, R. Lang, B. Lommel, K. Miernik, D. Miller, K. J. Moody, K. Morita, K. Nishio, A. G. Popeko, J. B. Roberto, J. Runke, K. P. Rykaczewski, S. Saro, C. Scheidenberger, H. J. Schött, D. A. Shaughnessy, M. A. Stoyer, P. Thörle-Pospiech, K. Tinschert, N. Trautmann, J. Uusitalo, and A. V. Yeremin, The European Physical Journal A **52**, 180 (2016)

[24] K. Morita, Nuclear Physics A **944**, 30 (2015)

[25] K. E. Gregorich, J. M. Gates, Ch. E. Düllmann, R. Sudowe, S. L. Nelson, M. A. Garcia, I. Dragojević, C. M. Folden III, S. H. Neumann, D. C. Hoffman, and H. Nitsche, Phys. Rev. C **74**, 044611 (2006)

[26] J. Dvorak, W. Brüchle, M. Chelnokov, R. Dressler, Ch. E. Düllmann, K. Eberhardt, V. Gorshkov, E. Jäger, R. Krücken, A. Kuznetsov, Y. Nagame, F. Nebel, Z. Novackova, Z. Qin, M. Schädel, B. Schausten, E. Schimpf, A. Semchenkov, P. Thörle, A. Türler, M. Wegrzecki, B. Wierczinski, A. Yakushev, and A. Yeremin, Phys. Rev. Lett. **97**, 242501 (2006)

[27] D. Peterson, B. B. Back, R. V. F. Janssens, T. L. Khoo, C. J. Lister, D. Seweryniak, I. Ahmad, M. P. Carpenter, C. N. Davids, A. A. Hecht, C. L. Jiang, T. Lauritsen, X. Wang, S. Zhu, F. G. Kondev, A. Heinz, J. Qian, R. Winkler, P. Chowdhury, S. K. Tandel, and U. S. Tandel, Phys. Rev. C **74**, 014316 (2006)

[28] S. Hofmann, S. Heinz, R. Mann, J. Maurer, G. Münzenberg, S. Antalic, W. Barth, L. Dahl, K. Eberhardt, R. Grzywacz, J. H. Hamilton, R. A. Henderson, J. M. Kenneally, B. Kindler, I. Kojouharov, R. Lang, B. Lommel, K. Miernik, D. Miller, K. J. Moody, K. Morita, K. Nishio, A. G. Popeko, J. B. Roberto, J. Runke, K. P. Rykaczewski, C. Scheidenberger, D. A. Shaughnessy, M. A. Stoyer, P. Thörle-Pospiech, K. Tinschert, N. Trautmann, J. Uusitalo, and A. V. Yeremin, The European Physical Journal A **52**, 116 (2016)

[29] F. P. Heßberger, The European Physical Journal A **53**, 75 (2017)

[30] J. Khuyagbaatar, H. Brand, R. A. Cantemir, Ch. E. Düllmann, F. P. Heßberger, E. Jäger, B. Kindler, J. Krier, N. Kurz, B. Lommel, B. Schausten, and A. Yakushev, Phys. Rev. C **104**, L031303 (2021)

[31] D. S. Delion, A. Insolia, and R. J. Liotta, Phys. Rev. C **46**, 1346 (1992)

[32] D. S. Delion, A. Insolia, and R. J. Liotta, Phys. Rev. C **46**, 884 (1992)

[33] R. Lovas, R. Liotta, A. Insolia, K. Varga, and D. Delion, Physics Reports **294**, 265 (1998)

[34] O. A. P. Tavares, S. B. Duarte, O. Rodríguez, F. Guzmán, M. Gonçalves, and F. García, Journal of Physics G: Nuclear and Particle Physics **24**, 1757 (1998)

[35] D. T. Akrawy, K. P. Santhosh, and H. Hassanabadi, Phys. Rev. C **100**, 034608 (2019)

[36] R. Smolańczuk, J. Skalski, and A. Sobiczewski, Phys. Rev. C **52**, 1871 (1995)

[37] R. Smolańczuk, Phys. Rev. C **56**, 812 (1997)

[38] M. Warda and J. L. Egido, Phys. Rev. C **86**, 014322 (2012)

[39] A. Staszczak, A. Baran, and W. Nazarewicz, Phys. Rev. C **87**, 024320 (2013)

[40] T. Ichikawa, A. Iwamoto, and P. Möller, Phys. Rev. C **79**, 014305 (2009)

[41] P. Jachimowicz, M. Kowal, and J. Skalski, Phys. Rev. C **101**, 014311 (2020)

[42] S. Giuliani, L. Robledo, and R. Rodriguez-Guzman, Phys. Rev. C **90**, 054311 (2014)

[43] W. J. Swiatecki, Phys. Rev. **100**, 937 (1955)

[44] D. W. Dorn, Phys. Rev. **121**, 1740 (1961)

[45] V. E. Viola Jr. and G. T. Seaborg, Journal of Inorganic and Nuclear Chemistry **28**, 741 (1966)

[46] Z. Ren and C. Xu, Nuclear Physics A **759**, 64 (2005)

[47] C. Xu and Z. Ren, Phys. Rev. C **71**, 014309 (2005)

[48] C. Xu, Z. Ren, and Y. Guo, Phys. Rev. C **78**, 044329 (2008)

[49] K. P. Santhosh, R. K. Biju, and S. Sahadevan, Nuclear Physics A **832**, 220 (2010)

[50] A. V. Karpov, V. I. Zagrebaev, Y. Martinez Palenzuela, L. Felipe Ruiz, and W. Greiner, International Journal of Modern Physics E **21**, 1250013 (2012)

[51] A. Zdeb, M. Warda, and K. Pomorski, Physica Scripta **89**, 054015 (2014)

[52] X. J. Bao, S. Q. Guo, H. F. Zhang, Y. Z. Xing, J. M. Dong, and J. Q. Li, Journal of Physics G: Nuclear and Particle Physics **42**, 085101 (2015)

[53] K. P. Santhosh and C. Nithya, Phys. Rev. C **94**, 054621 (2016)

[54] Z. Yuan, D. Bai, Z. Wang, and Z. Ren, The European Physical Journal A **60**, 68 (2024)

[55] A. V. M. Babu, N. Dhananjaya, H. C. Manjunatha, N. Sowmya, and A. M. Nagaraja, Modern Physics Letters A **39**, 2450018 (2024)

[56] A. Parkhomenko and A. Sobiczewski, Acta Phys. Polon. B **36**, 3095 (2005)

[57] E. V. Vladimirova, B. S. Ishkhanov, M. V. Simonov, S. V. Sidorov, and T. Yu. Tretyakova, International Journal of Modern Physics E **30**, 2150025 (2021)

CPC Accepted

[58] N. S. Moiseev, N. V. Antonenko, and G. G. Adamian, Phys. Rev. C **112**, 034607 (2025)
[59] N. Moiseev, N. Antonenko, and G. Adamian, Physics of Atomic Nuclei **88**, 831 (2025)
[60] J. Dong, W. Zuo, and W. Scheid, Phys. Rev. Lett. **107**, 012501 (2011)
[61] S. Cheng, Z. Ge, L. Cao, and F.-S. Zhang, Journal of Physics G: Nuclear and Particle Physics **48**, 095106 (2021)
[62] M. Wang, W. J. Huang, F. G. Kondev, G. Audi, and S. Naimi, Chinese Physics C **45**, 030003 (2021)
[63] P. Jachimowicz, M. Kowal, and J. Skalski, Atomic Data and Nuclear Data Tables **138**, 101393 (2021)
[64] H. J. Krappe, J. R. Nix, and A. J. Sierk, Phys. Rev. C **20**, 992 (1979)
[65] H. Huang, W. Zhang, A. Andreyev, Z. Liu, D. Seweryniak, Z. Li, C. Guo, A. Barzakh, P. Van Duppen, B. Andel, S. Antalic, M. Block, A. Bronis, M. Carpenter, P. Copp, J. Cubiss, B. Ding, D. Doherty, Z. Favier, F. Giacoppo, T. Huang, B. Kindler, F. Kondev, T. Lauritsen, J. Li, G. Li, B. Lommel, H. Lu, M. Al Monthery, P. Moša*checkmt*, Y. Niu, C. Raison, W. Reviol, G. Savard, S. Stolze, G. Wilson, H. Wu, Z. Wang, F. Xu, Q. Zeng, X. Yu, F. Zeng, and X. Zhou, Physics Letters B **833**, 137345 (2022).
[66] P. Brionnet, A. Lopez-Martens, O. Dorvaux, Z. Asfari, M. L. Chelnokov, V. I. Chepigin, H. Faure, B. Gall, K. Hauschild, A. V. Isaev, I. N. Izosimov, A. A. Kuznetsova, O. N. Malyshev, R. S. Mukhin, J. Piot, A. G. Popeko, Yu. A. Popov, K. Rezynkina, B. Sailaubekov, E. A. Sokol, A. I. Svirikhin, M. S. Tezekbayeva, A. V. Yeremin, and N. I. Zamyatin, Phys. Rev. C **112**, 014320 (2025)
[67] C. M. Folden III, I. Dragojević, Ch. E. Düllmann, R. Eichler, M. A. Garcia, J. M. Gates, S. L. Nelson, R. Sudowe, K. E. Gregorich, D. C. Hoffman, and H. Nitsche, Phys. Rev. C **79**, 027602 (2009)
[68] Nuclear spectroscopy in nuclei with $Z \geq 110$, Nuclear Physics A **944**, 376 (2015).
[69] Yu. Ts. Oganessian, V. K. Utyonkov, D. I. Solovyev, F. Sh. Abdullin, S. N. Dmitriev, D. Ibadullayev, M. G. Itkis, N. D. Kovrizhnykh, D. A. Kuznetsov, O. V. Petrushkin, A. V. Podshibiakin, A. N. Polyakov, A. G. Popeko, R. N. Sagaidak, L. Schlattauer, V. D. Shubin, M. V. Shumeiko, Yu. S. Tsyganov, A. A. Voinov, V. G. Subbotin, A. V. Sabelnikov, D. Abdusamadzoda, A. Yu. Bodrov, M. G. Voronyuk, G. A. Bozhikov, N. V. Aksenov, A. V. Khalkin, Z. G. Gan, Z. Y. Zhang, M. H. Huang, H. B. Yang, J. G. Wang, M. M. Zhang, and X. Y. Huang, Phys. Rev. C **113**, 014614 (2026)
[70] Yu. Ts. Oganessian, V. K. Utyonkov, F. Sh. Abdullin, S. N. Dmitriev, D. Ibadullayev, M. G. Itkis, A. V. Karpov, N. D. Kovrizhnykh, D. A. Kuznetsov, O. V. Petrushkin, A. V. Podshibiakin, A. N. Polyakov, A. G. Popeko, R. N. Sagaidak, V. V. Saiko, L. Schlattauer, V. D. Shubin, M. V. Shumeiko, D. I. Solovyev, Yu. S. Tsyganov, A. A. Voinov, V. G. Subbotin, A. V. Sabelnikov, D. Abdusamadzoda, A. Yu. Bodrov, M. G. Voronyuk, G. A. Bozhikov, N. V. Aksenov, A. V. Khalkin, Z. G. Gan, Z. Y. Zhang, M. H. Huang, H. B. Yang, J. G. Wang, M. M. Zhang, and X. Y. Huang, Phys. Rev. C **112**, 014603 (2025)
[71] Z. G. Gan, J. S. Guo, X. L. Wu, Z. Qin, H. M. Fan, X. G. Lei, H. Y. Liu, B. Guo, H. G. Xu, R. F. Chen, C. F. Dong, F. M. Zhang, H. L. Wang, C. Y. Xie, Z. Q. Feng, Y. Zhen, L. T. Song, P. Luo, H. S. Xu, X. H. Zhou, G. M. Jin, and Z. Ren, The European Physical Journal A-Hadrons and Nuclei **20**, 385 (2004)
[72] V. K. Utyonkov, N. T. Brewer, Yu. Ts. Oganessian, K. P. Rykaczewski, F. Sh. Abdullin, S. N. Dmitriev, R. K. Grzywacz, M. G. Itkis, K. Miernik, A. N. Polyakov, J. B. Roberto, R. N. Sagaidak, I. V. Shirokovsky, M. V. Shumeiko, Yu. S. Tsyganov, A. A. Voinov, V. G. Subbotin, A. M. Sukhov, A. V. Karpov, A. G. Popeko, A. V. Sabel'nikov, A. I. Svirikhin, G. K. Vostokin, J. H. Hamilton, N. D. Kovrizhnykh, L. Schlattauer, M. A. Stoyer, Z. Gan, W. X. Huang, and L. Ma, Phys. Rev. C **97**, 014320 (2018)
[73] S. Antalic, F. P. Heßberger, S. Hofmann, D. Ackermann, S. Heinz, B. Kindler, I. Kojouharov, P. Kuusiniemi, M. Leino, B. Lommel, R. Mann, K. Nishio, Š.. Šáro, B. Streicher, B. Sulignano, and M. Venhart, The European Physical Journal A **38**, 219 (2008)
[74] Yu. Ts. Oganessian, F. Sh. Abdullin, C. Alexander, J. Binder, R. A. Boll, S. N. Dmitriev, J. Ezold, K. Felker, J. M. Gostic, R. K. Grzywacz, J. H. Hamilton, R. A. Henderson, M. G. Itkis, K. Miernik, D. Miller, K. J. Moody, A. N. Polyakov, A. V. Ramayya, J. B. Roberto, M. A. Ryabinin, K. P. Rykaczewski, R. N. Sagaidak, D. A. Shaughnessy, I. V. Shirokovsky, M. V. Shumeiko, M. A. Stoyer, N. J. Stoyer, V. G. Subbotin, A. M. Sukhov, Yu. S. Tsyganov, V. K. Utyonkov, A. A. Voinov, and G. K. Vostokin, Phys. Rev. C **87**, 054621 (2013)
[75] S. Antalic, F. Heßberger, D. Ackermann, S. Heinz, S. Hofmann, B. Kindler, J. Khuyagbaatar, B. Lommel, and R. Mann, The European Physical Journal A **51**, 1 (2015)
[76] S. L. Nelson, K. E. Gregorich, I. Dragojević, M. A. Garcia, J. M. Gates, R. Sudowe, and H. Nitsche, Phys. Rev. Lett. **100**, 022501 (2008)
[77] F. P. Hessberger, Journal of Physics G: Nuclear and Particle Physics **25**, 877 (1999)
[78] Yu. Ts. Oganessian, V. K. Utyonkov, F. Sh. Abdullin, S. N. Dmitriev, R. Graeger, R. A. Henderson, M. G. Itkis, Yu. V. Lobanov, A. N. Mezentsev, K. J. Moody, S. L. Nelson, A. N. Polyakov, M. A. Ryabinin, R. N. Sagaidak, D. A. Shaughnessy, I. V. Shirokovsky, M. A. Stoyer, N. J. Stoyer, V. G. Subbotin, K. Subotic, A. M. Sukhov, Yu. S. Tsyganov, A. Türler, A. A. Voinov, G. K. Vostokin, P. A. Wilk, and A. Yakushev, Phys. Rev. C **87**, 034605 (2013)
[79] S. Hofmann, Status and prospects of synthesizing superheavy elements, in *Exotic Nuclei and Atomic Masses*, edited by J. Äystö, P. Dendooven, A. Jokinen, and M. Leino (Springer Berlin Heidelberg, Berlin, Heidelberg, 2003) pp. 353–358.
[80] R. Smolanczuk and A. Sobiczewski, Shell effects in the properties of heavy and superheavy nuclei, in *Low Energy Nuclear Dynamics: Proceedings of the XV Nuclear Physics Divisional Conference*, edited by Yu. Ts. Oganessian, W. von Oertzen, and R. Kalpakchieva (World Scientific, Singapore, 1995) p. 313.
[81] P. Möller, A. J. Sierk, T. Ichikawa, and H. Sagawa, Atomic Data and Nuclear Data Tables **109-110**, 1 (2016)
[82] N. Wang, M. Liu, X. Wu, and J. Meng, Physics Letters B **734**, 215 (2014)
[83] N. Wang, Nuclear mass table with WS4 model, 10.13140/RG.2.2.13370.18887 (2014).
[84] R. Rodríguez-Guzmán, Y. M. Humadi, and L. M. Robledo, The European Physical Journal A **56**, 43 (2020)
[85] Yu. Ts. Oganessian, V. K. Utyonkov, Yu. V. Lobanov, F. Sh. Abdullin, A. N. Polyakov, R. N. Sagaidak, I. V. Shirokovsky, Yu. S. Tsyganov, A. A. Voinov, A. N.

CPC Accepted

Mezentsev, V. G. Subbotin, A. M. Sukhov, K. Subotic, V. I. Zagrebaev, S. N. Dmitriev, R. A. Henderson, K. J. Moody, J. M. Kenneally, J. H. Landrum, D. A. Shaughnessy, M. A. Stoyer, N. J. Stoyer, and P. A. Wilk, Phys. Rev. C **79**, 024603 (2009)

[86] https: //www.jinr.ru/wp-content/uploads/JINR Docs/Seven Year Plan of JINR for 2024-2030 eng.pdf (2023), Seven year plan for the development of JINR for 2024–2030.

[87] J. M. Gates, R. Orford, D. Rudolph, C. Appleton, B. M. Barrios, J. Y. Benitez, M. Bordeau, W. Botha, C. M. Campbell, J. Chadderton, A. T. Chemey, R. M. Clark, H. L. Crawford, J. D. Despotopulos, O. Dorvaux, N. E. Esker, P. Fallon, C. M. Folden, B. J. P. Gall, F. H. Garcia, P. Golubev, J. A. Gooding, M. Grebo, K. E. Gregorich, M. Guerrero, R. A. Henderson, R.-D. Herzberg, Y. Hrabar, T. T. King, M. Kireeff Covo, A. S. Kirkland, R. Krücken, E. Leistenschneider, E. M. Lykiardopoulou, M. McCarthy, J. A. Mildon, C. Müller-Gatermann, L. Phair, J. L. Pore, E. Rice, K. P. Rykaczewski, B. N. Sammis, L. G. Sarmiento, D. Seweryniak, D. K. Sharp, A. Sinjari, P. Steinegger, M. A. Stoyer, J. M. Szornel, K. Thomas, D. S. Todd, P. Vo, V. Watson, and P. T. Wooddy, Phys. Rev. Lett. **133**, 172502 (2024)

[88] J. Khuyagbaatar, A. Yakushev, C. E. Düllmann, D. Ackermann, L.-L. Andersson, M. Asai, M. Block, R. A. Boll, H. Brand, D. M. Cox, M. Dasgupta, X. Derkx, A. Di Nitto, K. Eberhardt, J. Even, M. Evers, C. Fahlander, U. Forsberg, J. M. Gates, N. Gharibyan, P. Golubev, K. E. Gregorich, J. H. Hamilton, W. Hartmann, R.-D. Herzberg, F. P. Heßberger, D. J. Hinde, J. Hoffmann, R. Hollinger, A. Hübner, E. Jäger, B. Kindler, J. V. Kratz, J. Krier, N. Kurz, M. Laatiaoui, S. Lahiri, R. Lang, B. Lommel, M. Maiti, K. Miernik, S. Minami, A. K. Mistry, C. Mokry, H. Nitsche, J. P. Omtvedt, G. K. Pang, P. Papadakis, D. Renisch, J. B. Roberto, D. Rudolph, J. Runke, K. P. Rykaczewski, L. G. Sarmiento, M. Schädel, B. Schausten, A. Semchenkov, D. A. Shaughnessy, P. Steinegger, J. Steiner, E. E. Tereshatov, P. Thörle-Pospiech, K. Tinschert, T. Torres De Heidenreich, N. Trautmann, A. Türler, J. Uusitalo, M. Wegrzecki, N. Wiehl, S. M. Van Cleve, and V. Yakusheva, Phys. Rev. C **102**, 064602 (2020)

[89] P. Brionnet, M. W. Bordeau, R. K. Grzywacz, H. Haba, D. Kaji, T. T. King, K. Morimoto, T. Niwase, K. P. Rykaczewski, S. Sakaguchi, H. Sakai, and Y. Yamanouchi, Journal of the Physical Society of Japan **95**, 064201 (2026)

[90] X. Y. Huang, Z. Y. Zhang, J. G. Wang, L. Ma, C. L. Yang, M. H. Huang, X. L. Wu, Z. G. Gan, H. B. Yang, M. M. Zhang, Y. L. Tian, Y. S. Wang, J. Y. Wang, Y. H. Qiang, G. Xie, S. Y. Xu, Z. Zhao, Z. C. Li, L. C. Sun, L. Zhu, X. Zhang, H. Zhou, F. Guan, Z. H. Li, W. X. Huang, Z. Qin, Y. Wang, X. J. Yin, Y. F. Cui, Z. W. Lu, Y. He, L. T. Sun, Z. Z. Ren, S. G. Zhou, V. K. Utyonkov, A. A. Voinov, Yu. S. Tsyganov, A. N. Polyakov, D. I. Solovyev, N. D. Kovrizhnykh, and M. V. Shumeiko, Chin. Phys. Lett. **43**, 010101 (2026)

[91] https://rscf.ru/project/25-42-00018/.

CPC Accepted